View metadata, citation and similar papers at core.ac.uk

brought to you by CORE

provided by Drexel Libraries E-Repository and Archives

Multi-Phase Switching in Distribution Grids with Unbalanced Loads and Distributed Energy Resources

A Thesis

Submitted to the Faculty

of

Drexel University

by

Nicole Urim Segal

in partial fulfillment of the

requirements for the degree

of

Master of Science in Electrical Engineering

September 2008

© Copyright 2008
Nicole Urim Segal. All Rights Reserved.

Acknowledgments

The author wishes to express her indebtedness to Dr. Karen Miu- Miller for her invaluable guidance in this investigation and for the opportunity to study and perform research at the Center for Electric Power Engineering (CEPE). The author would like to acknowledge Dr. Miu-Miller's commitment to her as a student and for the dedication that was expressed towards the progression of the author's Electrical Engineering education.

The author also wishes to thank Dr. Nwankpa and Dr. Fischl for serving on her thesis committee and for their suggestions pertaining to the thesis document.

Special thanks are extended to Hakkı Yeğingil for his continued encouragement and support without which this thesis would not be realized. The author would like to offer sincere appreciation to Keith Sevcik for his assistance throughout the development of this work.

Finally the author would like to express her gratitude to her grandparents, Dr. Alan Segal and Liddie Segal, her aunts, Dr. Jane Segal and Marjorie Segal, her brother Samuel, and sister Adina for their love, support, and understanding that enhanced her professional endeavors. This manuscript is dedicated to them.

Table of Contents

List of Tables

List of Figures

Abstract

Multi-Phase Switching in Distribution Grids with Unbalanced Loads
and Distributed Energy Resources
Nicole Urim Segal
Karen N. Miu-Miller, Ph.D.

Distributed Energy Resource integration is ongoing. A popular and government subsidized choice is solar power. These installations are often residential and/or small commercial in type; hence, single-phase. In addition, the locations of the installations are not controlled with respect to a system viewpoint. Consequently, the photovoltaic generators will contribute to network imbalance throughout the network. These unbalanced contributions were not originally planned for by electric distribution companies. Therefore, new techniques to balance networks across phases are needed. This work defines metrics to quantify the level of imbalance, proposes a new switch model, formulates a new multi-phase network reconfiguration problem to correct phase imbalance at bus and examines a switching algorithm to correct the phase imbalance at buses.

Chapter 1. Introduction

Distributed Energy Resource (DER) integration is ongoing. Renewable resources help add to the generation diversity of the system. This is beneficial to the system because diversity adds reliability to the system by ensuring power from different types of generators. A popular and government subsidized choice is solar power. From a distribution system standpoint, photovoltaics (PHVs) help reduce the residential load. However, existing software that generation and transmission organizations use to analyze transmission systems assumes that the load from the distribution network is balanced. While the assumption that the load is balanced has been acceptable or met through various control techniques, the load may become unbalanced with the addition of DER's onto the distribution grid.

This work proposes measures to quantify the level of imbalance and introduces a switching algorithm to correct the phase imbalance at buses. In [9], the level of imbalance was examined with respect to node voltages due to random installation of photovoltaic arrays (PHVs) onto the distribution grid. This thesis looks at voltage and other metrics. Then, it proposes the use of multi-phase switches to balance the present phases across buses. Here, present phases means electrically connected phases. The practicality of purchasing multi-phase switches to install on the distribution system, switch lifetimes and switch maintenance costs are taken into consideration.

In sections 1.2 and 1.3 the background and motivation for multi-phase switching in distribution systems with unbalanced loads (including PHVs) is presented. In the section 1.4 selected component models for multi-phase power flow are introduced. Section 1.5 discusses network reconfiguration. Existing load balancing methods are presented next.

1.1 Background

Existing methods for load balancing include adjusting transformer tap settings, capacitor placement, and performing network reconfiguration. Adjusting feeder transformer tap settings is a popular method currently in use. This is a straightforward solution for engineers and directly affects the voltage magnitude ($|V|$) at local buses. However, adjusting tap settings at feeder transformers will not necessarily balance $|V|$ at downstream buses. Other buses may become unbalanced after the feeder transformer tap settings are changed. As a result the severity of the systems level of imbalance could increase. The definition of the level of imbalance will be clarified in Chapter 2.

Capacitors are often placed in the distribution systems for the purpose of reactive power compensation and energy loss reduction [15]. Capacitors are less expensive to install than switches and thus could be used as a solution for balancing. Separate capacitor banks are installed for phases A, B, and C. This is an advantage because each bank could potentially be turned off and on to balance individual phases. Yet, similar to network switches, the deployed control circuitries for the banks are predominately three phase.

However, the placement and control of capacitors is a complex problem and includes determining the location, size, and control schemes. Thus to simplify matters, many capacitors operate on a time-of-day algorithm (e.g. 7 am turn on 7 pm turn off) [15]. This is not conducive to distributed energy resources (DER) such as PHVs that are a function of time, irradiance, and temperature. In addition, capacitors are often treated as reactive power sources. Reactive power sources primarily affect $|V|$ at a bus and indirectly the current magnitude ($|I|$) at a branch. This acts as a disadvantage when DER's are added to the system. For residential PHVs the model used is mainly based on real power (P) and $|I|$; $|I|$ is controlled by a current controlled inverter [9]. Micro-turbines can be modeled as a P $|V|$ source. Adding capacitors to the system would increase reactive power (Q), which would increase $|V|$ at a bus. Thus, the expected increase in $|V|$ may cause over-voltage problems at system nodes.

Performing switch operations directly affects apparent power ($|S|$) and $|I|$ at a branch. This is an advantage because PHVs are mainly real power (P) injections. The reactive power (Q) is estimated from the constant power factor and generated real direct current (DC) power [9]. Also, the switches in the distribution system are commonly located downstream from the feeder buses. Therefore it is possible to balance buses that are further downstream from the feeders. However a disadvantage is the existing distribution systems contain mostly three phase (3Φ) switches. Still, it is important to investigate whether it is effective to upgrade and install select multi-phase switches in order to balance the individual phases A, B, and C.

The method of balancing chosen for this thesis is switching. The importance of maintaining a balanced network is described in the next section.

1.2 Motivation

Some types of loads and their performance are highly dependent on balanced voltages or balanced service from distribution companies. Specifically motor loads will be highlighted. Inherent characteristics of imbalance in distribution systems and DER will be reviewed.

1.2.1 Negative Effects of Imbalance on Machines

A significant amount of the loads in the distribution system are three-phase synchronous or induction motors. A high level of imbalance on motor loads can lead to the following undesirable effects:

- Unbalanced rotation
- Thermal stresses and reduced motor lifetime
- Delayed time to achieve optimal torque

Three-phase motors are built to receive balanced power which results in uniform rotation. An unbalanced input leads to physical stresses on 3φ machines. The American National Standards Institution (ANSI), Standard C84.1-2006 Annex 1, and National Electric Machines Association (NEMA) define a maximum voltage imbalance as 5% [1].

In [18, 19] the impacts of machines voltage imbalance were examined. It was indicated that when voltage imbalance reaches 5%, machine temperature increased rapidly. The machine cannot be protected from damage due to the increase in temperature. Also, with unbalanced voltages the motor will take a longer time to reach the optimal torque. Thus thermal stresses on the motor increase which will lead to the motor's "loss of life," and possibly result in failure of the machine. In addition, a reduced net torque is seen from the imbalance. This will cause the machine to operate at a higher slip when operating with a full load. The higher slip will increase the rotor losses thus causing greater heat dissipation. Unbalanced voltage increases the temperature of the stator winding. This also leads to a loss of motor life.

Distribution systems are unbalanced as a result of the loads and by physical construction of some feeders, which are single and two-phase. The effect on the network and power flow is presented in the next section.

1.2.2 Unbalanced Network Components

Unbalanced flows are a significant concern in a distribution system with a large number of open-delta/open-Y transformer connections [26]. For example a variety of problems, such as, an unbalanced voltage profile due to unbalanced voltage drops, and degradation of the system efficiency can result. Another adverse effect caused by a high level of imbalance on the loads is the possible overuse of one or a group of system transformers.

This may occur because the power drawn on one phase of a feeder will be greater than another phase.

This thesis focuses on PHV generation. However, the problem formulation and solution algorithm relate to all other single-phase DERs. PHVs contribute to network imbalance for several reasons. Networks contain small load changes such as lights turning off and on and powering on and off machines. These small changes will result in small differences in the voltages. PHVs effectively reduce load on bus locations when they are operating and may contain advanced control and interconnection devices. As a result of the PHVs, changes in voltage may no longer be small.

A 20% residential load reduction from solar generators is expected by PSE&G solar loan program by the year 2020 [33]. AEC has committed to a 20% load reduction by renewable resources by the year 2020 [34]. The state of New Jersey currently has 5.5% of its generated power from renewable resources [35].

Also, PHV installations are predominately single-phase and electric distribution companies do not control the installation location. Additionally, the dynamic power output of the PHV varies as a function of solar irradiance and ambient temperature.

Thus, control of the level of system imbalance is needed because of:

1. Grid integrated distributed energy resources
2. The need for balanced power and voltage to be supplied to the load

Consequently the level of imbalance must be quantified. This concept is discussed in Chapter 2. Select component models that are used in this thesis are presented in the next section.

1.3 Select Component Models

The typical components of a three-phase network include generators, transformers, loads, switches, lines, capacitors, and co-generators. The components can be single, two and three phase. This list has been expanded by [9] to include PHVs. Load, switch, and PHVs components are relevant to this thesis; a brief discussion of these models will follow. Additional distribution component models can be found in [31].

1.3.1 Load Models

The load models considered in the three-phase power flow include constant admittance (*Z*), constant current (*I*), and constant power (*PQ*) models. Linear combinations of these models are known collectively as ZIP models. The table below shows the loads expressed as currents, [31].

Table 1.1 Grounded WYE and Ungrounded Delta Load Models

Load Model	Grounded WYE	Ungrounded Delta
Constant *Z*	$I_{L,i} = -\left(\bullet \frac{S_{L,i}^{*}}{\left\| V_i \right\|^2} \right) V_i$	$I_{L,i} = -\begin{bmatrix} y_{L,i}^{CA} + y_{L,i}^{AB} & y_{L,i}^{CA} \\ -y_{L,i}^{AB} & y_{L,i}^{BC} \end{bmatrix} V_i$
Constant *I*	$I_{L,i} = -\left(\bullet \frac{S_{L,i}}{V_i} \right)^{*}$	$I_{L,i} = \begin{bmatrix} I_{L,i}^{CA} - I_{L,i}^{AB} \\ I_{L,i}^{AB} - I_{L,i}^{BC} \end{bmatrix}$
Constant *PQ*	$I_{L,i} = \left(\bullet \frac{S_{L,i}}{V_i} \right)^{*}$	$I_{L,i} = \begin{bmatrix} \frac{S_{L,i}^{AB}}{V_i^{AB}} - \frac{S_{L,i}^{CA}}{V_i^{AB} + V_i^{BC}} \\ \frac{S_{L,i}^{AB}}{V_i^{AB}} - \frac{S_{L,i}^{BC}}{V_i^{BC}} \end{bmatrix}^{*}$

In Table 1.1, dot division ($\bullet/$) indicates element wise division. $I_{L,i}$ and $S_{L,i}$ are respectively, the current injected by the load at bus i and apparent power injected by the load at bus i. In addition, in grounded connections node voltages are phase-to-ground voltages. Thus at bus i, corresponding voltage, current and power are complex (*3 x 1*) vectors.

$$V_i = \begin{bmatrix} V_i^A \\ V_i^B \\ V_i^C \end{bmatrix} \qquad (1.3.1)$$

where:

V_i: *Voltage to ground reference at bus i*

However, in ungrounded portions of the network and ungrounded loads, line-to-line voltage quantities are utilized with phase *CA* used as a reference. This results in (*2 x 1*) complex vectors.

$$V_i = \begin{bmatrix} V_i^{AB} \\ V_i^{BC} \end{bmatrix} \qquad (1.3.2)$$
$$V_i^{CA} = -\left(V_i^{BC} + V_i^{AB}\right)$$

In this thesis, single and two phase parameters are represented by replacing phases that are not present with zeros. Absent phases are represented with zeros to maintain the size of the data structures. The data structures are explained in detail in the solution algorithm chapter. The concept of replacing phases that are not present with zeros is also applied to switching. The next section presents the switching model for the system.

1.3.2 Switch Component Model

Two types of switches are used in the system. They are tie switches which are normally open switches, and sectionalizing switches which are normally closed switches. The purpose of the tie switch is to link neighboring network sections. The sectionalizing switch is used to clear faults or perform network reconfiguration. Traditional power flow solvers have modeled these as three-phase switches. Two states for a switch are closed and opened. Figure 1.1 below is an example of a three-phase switch in the closed and open states.

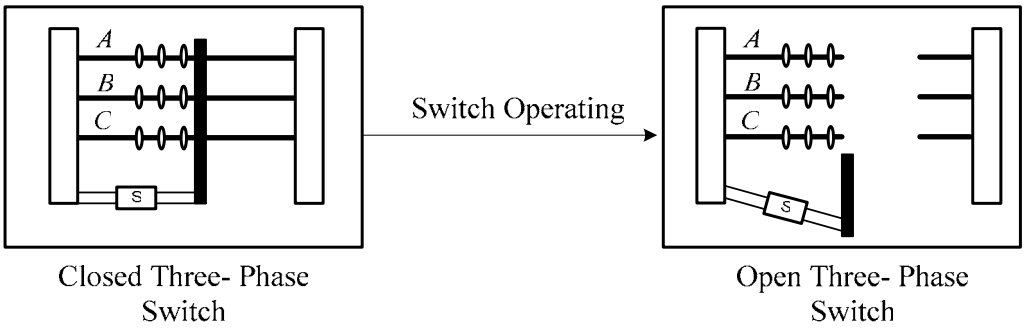

Figure 1.1 Three Phase Switch Model

A closed three-phase switch is shown on the left. An opened three phase switch is shown on the right. All phases in Figure 1.1 for a three-phase switch are closed or open. Phases of a three-phase switch cannot be operated individually. This thesis expands the model by creating a multi-phase switch model.

A multi-phase switch is a switch that permits each electrically connected phase of a switch to open and close individually. Each phase, *A*, *B*, and *C* of a multi-phase switch has its own closed and open states. Figure 1.2 below is a multi-phase switch in its six $\left(2^3\right)$ states. Please see Figure 1.2 below for an example.

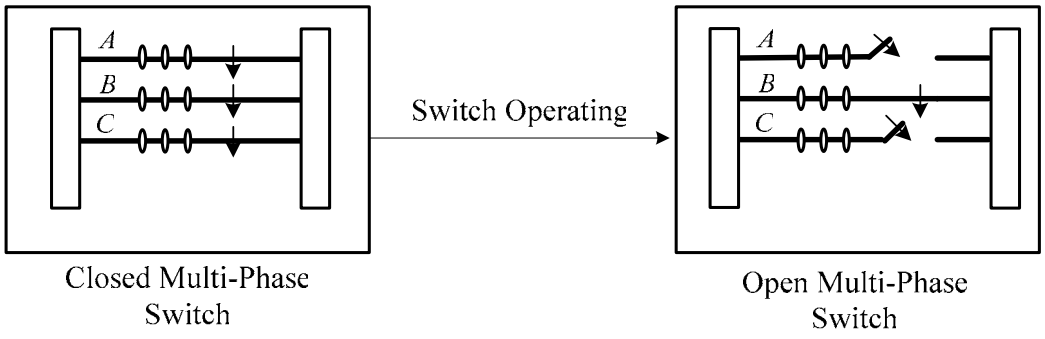

Figure 1.2 Multi-Phase Switch Model : E.g. Phase *A* and *C* Open

Figure 1.2, a multi-phase switch with phases *A*, *B*, and *C* closed is shown on the left, and, a multi-phase switch with phases *A* and *C* open is shown on the right. Phase *B* remains closed in this example of an open multi-phase switch. Details of this new switching capability and software implementation are presented in Chapter 3.

Throughout this thesis electrical parameters will be defined as shown in Figure 1.3 below.

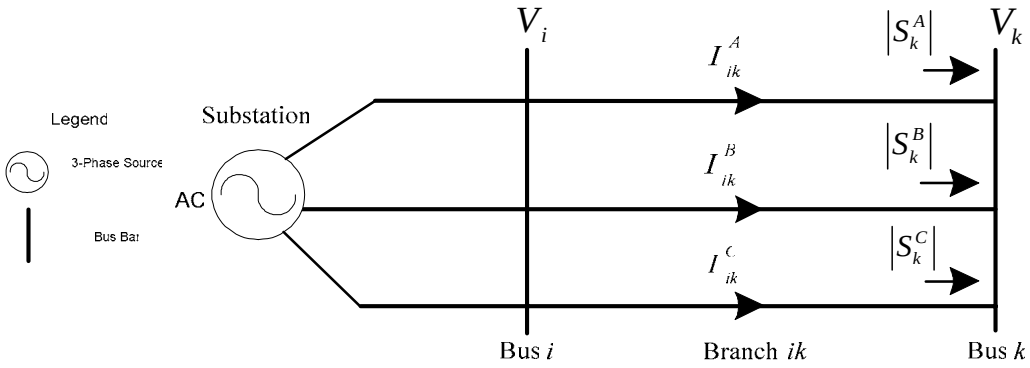

Figure 1.3 Electrical Parameters Defined for a Two Bus System

Figure 1.3 above shows the path of the current from the substation thru branch ik, the voltages at bus i, and bus k, and the apparent power injected into bus k. The substation is modeled as a three-phase AC source. The buses and branch are indicated by name and are bus i, bus k, and branch ik. The direction of current is indicated by arrows along branch ik. Mathematically I_{ik} is defined as:

$$I_{ik} = \begin{bmatrix} I_{ik}^A \\ I_{ik}^B \\ I_{ik}^C \end{bmatrix} \qquad (1.3.3)$$

where:

I_{ik} : *Current thru (in direction of) branch ik*

Mathematically $|S_k|$ is defined as:

$$|S_k| = \begin{bmatrix} |S_k^A| \\ |S_k^B| \\ |S_k^C| \end{bmatrix} \qquad (1.3.4)$$

where:

$|S_k|$: *Apparent Power at bus k*

Next, examples of source models that are found in a distribution network are described.

1.3.3 Sources

Three types of source bus models exist in traditional three-phase power flow solvers. They include *PQ*, *P*|*V*| and slack buses. The photovoltaic (PHV) generator model can generically be represented as a *PQ* or *P*|*V*| source. The PHV model that was selected from [9] behaves as a *PQ* source and is explained in the following section.

Photovoltaic (PHV) Model

The photovoltaic generators for residential and small commercial customers are smaller in size, e.g. <10kW [9], and generally from a system standpoint impact single and two-phase loads. A general PHV model for residential and small commercial customers was chosen to be a *PQ* model. The *PQ* model assumes a current control scheme that allows the PHV to provide a very high power factor with simple control circuitry [11]. The current voltage phase angle of the generator is made to match the voltage phase angle of the grid thus resulting in a high power factor. The high power factor and reduced costs in circuitry make this model ideal for residential and small commercial customers. Then, from [9], the *PQ* model is now discussed.

The DC power output generated by the PHV is dependent on the solar irradiance (G), ambient temperature (T) and time. Environmental conditions and 24-hour load curves have been automated. Modeling assumptions from [9] are listed below:

A1. In the model the efficiency of the machine η is constant.

A2. The output power is scaled in proportion to the efficiency.

A3. The power factor is 0.9 – 1

A4. The PHV array operates at the maximum power point thus supplying the maximum real power at given operational conditions (e.g. irradiance etc).

Finally, the source is then integrated into three-phase power flow by:

$$S_k^{inj} = S_{Lk}^{inj} + S_{Gk}^{inj} \qquad (1.3.5)$$

where:

$$\begin{aligned} &S_k^{inj} : \textit{total power injected at bus k} \\ &S_{Lk}^{inj} : \textit{power injected by the load at bus k} \\ &S_{Gk}^{inj} : \textit{power injected by the PHV at bus k} \end{aligned} \qquad (1.3.6)$$

A focus on the effects of residential PHV generation is selected in this thesis. Assuming the converter can maintain a specified power factor PHVs can be viewed as a complex power injection. Residential installations are often single-phase or two-phase installations. As such imbalance may be introduced with their installations and multi-phase switching is investigated. Thus, in the next section an overview of Network Reconfiguration (NR) is discussed.

1.4 Network Reconfiguration (NR)

Historically, there are three main reasons for performing network reconfiguration on a distribution system. They include service restoration [6, 7, 16, 28], load balancing [6, 7, 2, 3, 10, 12], and to reduce the power (I^2R) losses of the system [6, 7, 3, 13].

In service restoration, NR is conducted to isolate a faulted area, supply power to out of service customers (non-faulted), and minimize load shedding [16, 28]. In load balancing, NR is performed to relieve overloads on the feeders in the distribution system. There are various approaches and objectives presented for network reconfiguration. A common objective is to minimize the number of switch operations when reconfiguring the network.

The majority of the algorithms today use a combination of heuristics and search techniques, such as greedy search, and simulated annealing [6, 7] to alter the topology of the network. Although the network reconfiguration is used to achieve different goals, most papers, switch vendors and books [2, 3, 10, 12, 16, and 28] include common assumptions:

A1. The location of the load is known.

A2. The load is diversified.

Exceptions are presented in [10, 16, 14, 21, 22, and 23]. For example a heuristic search algorithm for changing loads is presented in [10]. The algorithm uses established load

patterns to determine the initial set of switch operations. However this practical approach does not incorporate independent phase switching. In addition this method works well only when the degree of imbalance is not very high [12]. In [16] load varying curves are used as an input to determine time based switch operations for service restoration. In [16] only out-of-service loads vary and three phase switching is employed. In [14, 21, 22] varying load models were developed for cold load pick up and again three-phase switching is employed.

1.5 Summary

This thesis presents a new category of network reconfiguration called phase balancing. Phase balancing is the act of performing switch operations to balance phases across a bus. Phase balancing is important because the majority of the loads on the distribution system are motors and the addition of distributed energy resources (DER) onto the grid is inevitable. Yet, certain types of distributed energy resources increase the imbalance among the phases because they are multi-phase installations with time and temperature dependence.

Thus this thesis will address the problem of multi-phase switching in distribution systems with uncertain loads (including PHV generation). This thesis presents a problem formulation and simulation results for phase balancing. Network reconfiguration will be utilized. The search algorithms that will be employed are the greedy search and memory based heuristics. Analytically determined indices for level of imbalance guide the search.

In the next chapter the problem formulation for the multi-phase switching with uncertain loads problem is presented.

Chapter 2. Problem Formulation

In this chapter, the multi-phase switching problem formulation is presented. The multi-phase switching problem is formulated to balance electrical parameters at a bus across its existing phases. The problem is formulated as a constrained, non-differentiable, multi-objective optimization problem. The problem formulation will only be applied if the initial power flow is unbalanced. In section 2.2, the metrics that are used to quantify the level of imbalance and a definition of imbalance is presented. In section 2.3, the objectives are presented and in section 2.4, the constraints are described.

2.1 Quantifying Levels of Imbalance

The level of imbalance can be viewed from different electrical parameters, e.g. apparent power and voltage magnitudes. In order to quantify the level, it is proposed to determine the average value across the present phases at a bus. Present phases are phases that are electrically connected and are in-service. The maximum difference of a parameter value from the average is defined to be the maximum phase difference from the average. The difference between the maximum phase difference from the average and a user inputted threshold identifies what phases at a bus would need correction. This difference is defined as the measure of imbalance. A flow chart reflecting the order in which the definitions will be presented and how the imbalance will be quantified is shown below in Figure 2.1.

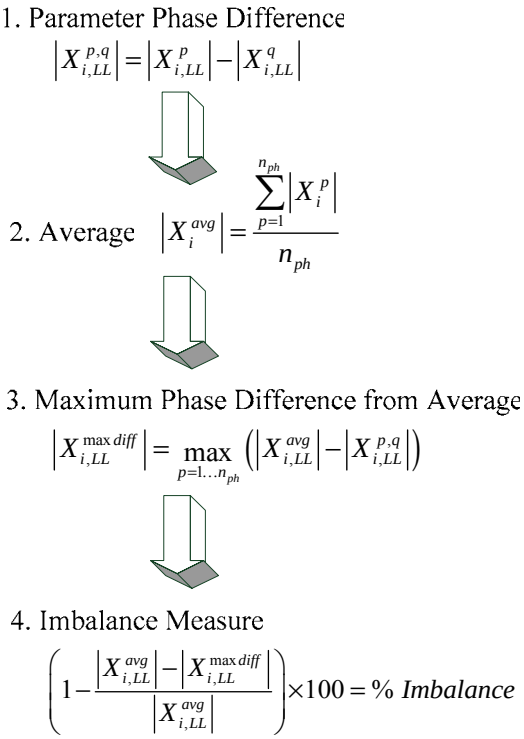

Figure 2.1 Flow Chart Defining Acceptable Levels of Imbalance

In this thesis, measures for the level of imbalance will be utilized with respect to voltage magnitude, $|V|$, current magnitude, $|I|$, and apparent power, $|S|$. X in Figure 2.1 above represents electrical parameters $|S|$, $|I|$, and $|V|$. In the next subsection, the ANSI voltage imbalance measure is described.

2.1.1 American National Standards Institution's (ANSI) Voltage Imbalance

The voltage imbalance measure comes from the ANSI, Standard C84.1-2006 Annex 1, the American National Standard for Electric Power Systems and Equipment—Voltage Ratings (60 Hertz). The annex discusses derating motor capacity at a 5% level of

imbalance. The standard describes the criterion for measuring imbalance using line-to-line voltages. It states "…the measurement (that is) specified is the difference between the average of the three phase magnitudes and the voltage that differs the most from that average, divided by the average (expressed as a percent) [1]." It is expressed as:

(2.1.1)

(2.1.2)

where:

$\left|V_i^{avg}\right|$: *The average phase voltage at bus i, computed as*:

$$\left|V_i^{avg}\right| = \frac{\sum_{p=1}^{n_{ph}} \left|V_i^{p}\right|}{n_{ph}} \qquad (2.1.3)$$

where:

p : *corresponding phases A, B, C*

n_{ph} : *total number of phases present at bus i*

and

$\left|V_i^{\max diff}\right|$: *The maximum difference of the average voltage and phase voltage at bus i, is computed as*:

$$\left|V_i^{\max diff}\right| = \max_{p=1\cdots n_{ph}} \left(\left|V_i^{avg}\right| - \left|V_i^{p}\right|\right) \qquad (2.1.4)$$

This concept has been expanded to include finding imbalance for the apparent power, $|S|$, and current magnitude, $|I|$ measurements. In equation 2.1.1 the maximum allowable imbalance defined with respect to voltage, is five percent and is from [1]. For this work, the maximum allowable imbalance will be discussed further in section 2.4.

2.1.2 Parameter Phase Difference $\left|X_{i,LL}^{p,q}\right|$

The parameter phase difference, X , at a bus i and for a load level LL, is $\left|X_{i,LL}^{p,q}\right|$ and is defined as:

$$\left|X_{i,LL}^{p,q}\right| = \left|X_{i,LL}^{p}\right| - \left|X_{i,LL}^{q}\right| \qquad (2.1.5)$$

where:

$X : |S|,\ |V|,$ or $|I|$

$\left|X_{i,LL}^{p,q}\right|$: *parameter phase difference between p and q at bus i and for LL*

$X_{i,LL}^{p}$: *phase p parameter at bus i and for LL*

$X_{i,LL}^{q}$: *phase q parameter at bus i and for LL*

p : *phase* $\{A,B,C\}$

q : *phase* $\{A,B,C\}$

LL : *load level*

Above in equation 2.1.5, $\left|S^{p,q}\right|, \left|I^{p,q}\right|$, and $\left|V^{p,q}\right|$ are the differences across the present phases at a bus. Only present phases are used to measure imbalance. A bus with a single phase present would be considered balanced since only one phase is present. Here, both $\left|S_i^{p,q}\right|$ and $\left|I_{\mathrm{i}}^{p,q}\right|$ are phase-to-phase values from the incoming branch at the present phases of a bus i. An example, of the $|V|$ phase difference at bus i, for a load level LL is:

$$\left|V_{i,LL}^{p,q}\right| = \left|V_{i,LL}^{p}\right| - \left|V_{i,LL}^{q}\right| \quad (2.1.6)$$

A load level can be defined by the distribution system planner or operator (e.g. levels such as light, medium, and heavy loads or hours) depending on the application. This thesis will focus on planning problems.

2.1.3 Average $\left|X_{i,LL}^{avg}\right|$

The second definition that is needed to quantify the imbalance measure is to define the average, $\left|X_{i,LL}^{avg}\right|$. The electrical parameter's average of at bus i and for a *LL* is defined as:

$$\left|X_i^{avg}\right| = \frac{\sum_{p=1}^{n_{ph}} \left|X_i^p\right|}{n_{ph}} \qquad (2.1.7)$$

Again the average is based only on the present phases at a bus i and for a load level *LL*.

where:

$\left|X_{i,LL}^{avg}\right|$: *the parameter's average of the present phases at bus i*

n_{ph} : *total number of phases present at bus i*

In the next section, the maximum phase difference from the average is defined.

2.1.4 Maximum Phase Difference from Average $\left|X_{i,LL}^{\max diff}\right|$

The maximum phase difference from the average, $\left|X_{i,LL}^{\max diff}\right|$, is defined as:

$$\left|X_{i,LL}^{\max diff}\right| = \max_{p=1\ldots n_{ph}} \left(\left|X_{i,LL}^{avg}\right| - \left|X_{i,LL}^{p,q}\right|\right) \qquad (2.1.8)$$

where:

$\left|X_{i,LL}^{\max diff}\right|$: *The maximum difference of the average and phase difference at bus i*

For example, the maximum phase difference for |*V*| at bus i and for a load level *LL* is:

$$\left|V_{i,LL}^{\max diff}\right| = \max_{p=1\cdots n} \left(\left|V_{i,LL}^{avg}\right| - \left|V_{i,LL}^{p,q}\right|\right) \qquad (2.1.9)$$

2.1.5 Imbalance Measure % *Imbalance*

Using all prior metrics the measure of imbalance from the average is defined as:

$$\left(1-\frac{\left|X_{i,LL}^{avg}\right|-\left|X_{i,LL}^{\max diff}\right|}{\left|X_{i,LL}^{avg}\right|}\right)\times 100 = \%\ Imbalance \quad (2.1.10)$$

The measure of $|V|$ imbalance from the average at bus i and for a load level LL is:

$$\left(1-\frac{\left|V_{i,LL}^{avg}\right|-\left|V_{i,LL}^{\max diff}\right|}{\left|V_{i,LL}^{avg}\right|}\right)\times 100 = \left|V_{i,LL}\right|\ \%\ Imbalance \quad (2.1.11)$$

The measure of imbalance from the average for phase balancing is unlike [1] because it examines the parameter phase difference defined as the difference between the present phases at a bus. This is an important difference because in [1] it was assumed that all three phases at a bus were present. As a result of using present phases at a bus, different switching schemes will result in different power system operating points. An example of how imbalance measure is considered is shown in the next section.

2.1.6 Imbalance Measure Example

A 2-bus case is used as an example of determining the imbalance measure. The 2-bus case is displayed in Figure 2.2 below.

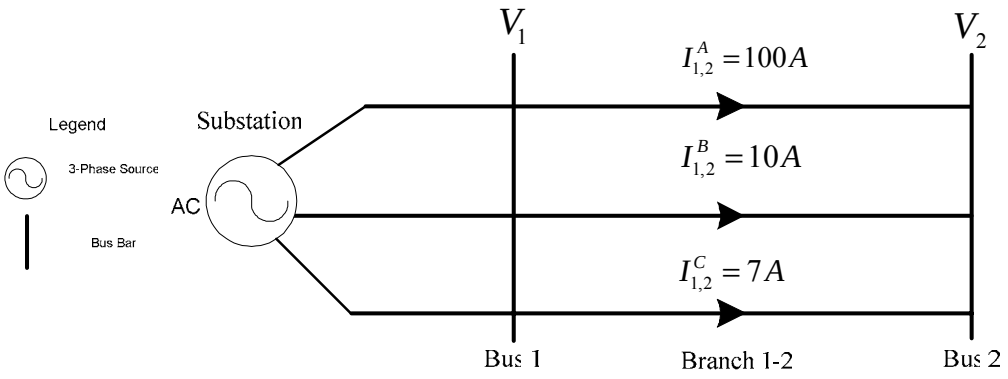

Figure 2.2 Two Bus Case Example using Current Magnitude

Figure 2.2 above has a 3-Φ source, and two buses, *bus* 1 and *bus* 2. The current magnitude at each phase of *branch* 1-2 is shown.

Table 2.1 Current Magnitude for Branch 1-2

	|*I*| (Amps)		
Branch	**A**	**B**	**C**
1-2	100	10	7

Here, current magnitude was chosen to illustrate the first step of finding the imbalance measure. The first step is to find the current magnitude phase difference for *bus* 2. Table 2.2 shows the per unit magnitude difference at *bus* 2 and for phase differences *AB*, *BC*, and *CA*.

Table 2.2 |*I*| Phase Difference for Bus *2*

	|*I*| Phase Difference (Amps)		
Bus	**AB**	**BC**	**CA**
2	90	3	93

In Table 2.2, the minimum |*I*| magnitude phase difference occurs for *BC*. Phases *AC* and *CA* have the largest phase differences. The common phase *A* indicates the imbalanced phase. Secondly, the average across the present phases of a bus is determined.

Table 2.3 Average |*I*| for Bus *2*

Bus	**|*I*| Average (Amps)**
2	39

Table 2.3 above gives the average at the present phases of *bus* 2 . The next step in finding the |*I*| % imbalance is to calculate the maximum phase difference from the average.

Table 2.4 |*I*| Phase Difference from Average for Bus *2*

	|*I*| Phase Difference from Average (Amps)			
Bus	**Avg - AB**	**Avg - BC**	**Avg - CA**	**MAX**
2	51	36	54	54

Table 2.4 above lists the |*I*| phase differences from the average for *bus* 2 . The fifth column lists the maximum of the phase differences *AB*, *BC*, and *CA* . The maximum |*I*|

phase differences from the average are identified at *bus* 2 phase *CA* and bus *2* phase *AB*. *A* is the common phase and therefore is considered the unbalanced phase.

Another method would be to compute the parameter % imbalance using the difference between current at phases *A*, *B*, and *C* and the average. The |*I*| difference from the average for *bus* 2 .

Table 2.5 |*I*| Difference from Average for Bus *2*

	|*I*| Difference from Average (Amps)			
Bus	**Avg - A**	**Avg - B**	**Avg - C**	**MAX**
2	61	29	32	61

Using this method phase *A* is identified as the imbalanced phase. The difference between the average and phase *A* is 61 A, this value in comparison to the average value 39 A is a difference of 22 A. The difference between the average and phase *C* is 32 A, this value in comparison to the average value 39 A is a difference of 7 A. Phases *A* and C appear to be closer in value. However, using Table 2.2 the phase difference *CA* is 93 A. In this thesis the phase difference is chosen. Lastly, the |*I*| % imbalance is found.

Table 2.6 gives the |*I*| % imbalance at *bus* 2 for the 2-Bus example.

Table 2.6 $|I|$ % Imbalance for Bus *2*

Bus	$\|I\|$ % Imbalance
2	138

In the table above the $|I|$ percent imbalance at each bus is displayed. The percent imbalance for *bus* 2 is 138 %. This percent imbalance is greater than 100 % this example is extremely unlikely but would indicate that phase balancing should be performed. The amount of percent imbalance that is necessary for phase balancing will be discussed in section 2.4.2.

Another method for measuring the % imbalance would be to compute the average of the phase differences. In this example voltage magnitude was chosen to illustrate finding the imbalance measure.

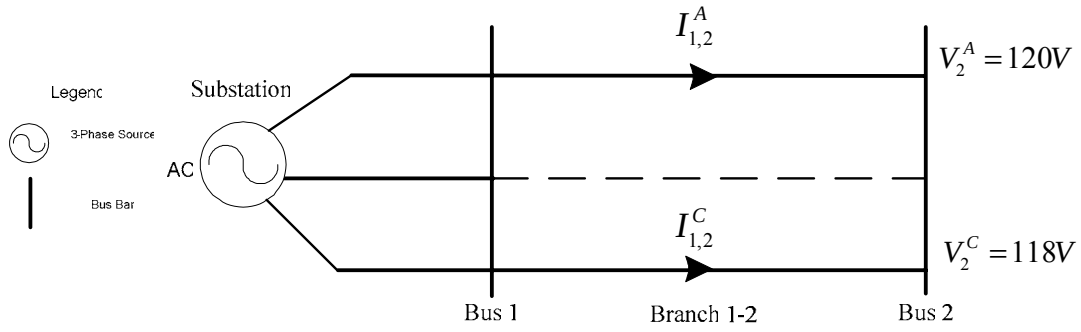

Figure 2.3 Two Bus Case Example Using Voltage Magnitude

Figure 2.3 above has a 3-Φ source, and two buses, *bus* 1 and *bus* 2. The voltage magnitude at each electrically connected phase of *bus* 2 is shown. Phase B is not

connected which is indicated by a dashed line. The phase difference, AB, for *bus* 2 equals *2* and the average for phases A and B is 119 *V*.

Averaging the phase differences would result in $\frac{AB}{1}$. Thus, averaging the phase differences for a bus with two present phases is the phase difference. This method is not applicable for buses with two present phases because no parameter % imbalance can be determined. Therefore, the average was chosen over the average of the phase differences in order to compute the parameter % imbalance.

In the next section, the objectives for the multi-phase switching problem are presented.

2.2 Objectives

The primary objective for the multi-phase switching problem is to minimize the total cost of purchasing, installing and maintaining new and existing multi-phase switchgear on the distribution grid for the purpose of phase balancing. Additional objectives include minimizing the cost of maintaining existing switch gear. Mathematically, the problem can be defined as:

$$\min_{g_k} C_{pi}(n_{sw}^{n}(g_k^0, g_k)) + C_m(n_{sw}^{n}(g_k^0, g_k) + n_{sw}^{e}(g_k^0, g_k)) \quad (2.2.1)$$

where:

$g_k^0 = \left[g_k^{0(A)} \quad g_k^{0(B)} \quad g_k^{0(C)} \right]$: initial switch settings,
Discrete (0- open, 1-closed)

$g_k = \left[g_k^A \quad g_k^B \quad g_k^C \right]$: proposed set of sectionalizing & tie switches,
Discrete (0- open, 1-closed)

$n_{total}(g_k^0, g_k) = n_{sw}^n + n_{sw}^e$: Total number of open/close switch operations

$n_{sw}^n(g_k^0, g_k)$: Number of new open/close switch operations

$n_{sw}^e(g_k^0, g_k)$: Number of existing open/close switch operations

$C_{pi}\left(n_{sw}^n\right)$: cost of purchasing & installing switches

$C_m\left(n_{sw}^n + n_{sw}^e\right)$: cost of maintaining new and existing switches

The maximum total size of the search space is all possible configurations for a switch at each load level or $g_k = \left(2^{n \times 3}\right) \times n_{LL}$. Here *2* represents the two statuses of a switch (open or close), *n* is the number of switches, *3* is for all possible phases *A, B,* and *C*, and n_{LL} is the number of load levels.

As a result of using multi-phase switching the size of the network reconfiguration problem increases to n_{buses} *x 3*. For example, a three phase switch operating using bus structure has only two switch statuses, open and close ($2^1 = 2$). The same multi-phase switch can have six switch statuses ($2^3 = 6$) or two statuses per phase. Here, for practical implementation reasons the search space with respect to *n* will be limited to include only same phase-to-same phase switching. For example, Phase *A*- Phase *A* switching is allowed, but Phase *A*- Phase *B* switching is not allowed. Also, for planning purposes the number of load levels is often limited to a set of loading profiles (high, medium, and low) and can be dictated by the distribution system planner.

Although the complexity of the problem has increased, it is necessary to change switching models. These alterations impact subsequently analysis tools and this will be discussed in Chapter 3. In the following section, the constraints of the problem are described.

2.3 Operational Constraints

The inequality and equality constraints define guidelines to finding a solution that is feasible, i.e. will remain within system operating limits.

2.3.1 Equality Constraints

The equality constraint is that unbalanced power flow must be satisfied. This is required for all load levels in order for the solution to be realistic and provide an accurate model of the state of the distribution system. Mathematically, this is stated as:

$$F_{LL}\left(g_k\right)=0 \quad LL=1\cdots n_{LL} \quad (2.3.1)$$

The power flow equations, *F*, are a set of non-linear algebraic equations and the solution provides the steady state voltages at each node in a system. In the next section the inequality constraints are presented.

2.3.2 Inequality Constraints

Two main types of inequality constraints are identified. First, inequality constraints require the system to be within the electrical and thermal operating limits. Second, the operating point should be balanced or within an acceptable level of imbalance. The three electrical and thermal inequality constraints considered are current, voltage, and apparent power constraints.

Some notation is first listed:

n_{branch} : *number of energized branches*
n_{bus} : *number of buses*
n_{LL} : *number of load levels*
$I_k = \left[I_k^A \quad I_k^B \quad I_k^C \right]^T$: *Current thru branch k*
$V_i = \left[V_i^A \quad V_i^B \quad V_i^C \right]^T$: *Voltage at bus i*
$\left|S_i\right| = \left[\left|S_i^A\right| \quad \left|S_i^B\right| \quad \left|S_i^C\right| \right]^T$: *Apparent power at bus i*
$P_i = \left[P_i^A \quad P_i^B \quad P_i^C \right]^T$: *Real power at bus i*
$Q_i = \left[Q_i^A \quad Q_i^B \quad Q_i^C \right]^T$: *Reactive power at bus i*

The current constraint is defined as:

$$\left|I_{k,LL}\right| \le \left|I_{k,LL}^{\max}\right| \quad \forall \quad k \in \text{ all energized branches}, \quad \forall \quad LL = 1 \cdots n_{LL} \tag{2.3.2}$$

Here k is a branch in the set of all energized branches (i.e. $k = 1 \ldots n_{branch}$). $\left|I_{k,LL}\right|$ is the current across a branch k. $\left|I_{k,LL}^{\max}\right|$ is the maximum acceptable current magnitude on branch k. This constraint is required for all load levels.

The voltage constraint is defined as:

$$\left|V_{i,LL}^{\min}\right| \le \left|V_{i,LL}\right| \le \left|V_{i,LL}^{\max}\right| \quad \forall \quad i \in \textit{all energized buses}, \quad \forall \quad LL = 1 \cdots n_{LL} \tag{2.3.3}$$

Here i is a bus in the set of all energized buses (i.e. $i = 1 \ldots n_{bus}$). The $\left|V_{i,LL}^{\min}\right|$ and $\left|V_{i,LL}^{\max}\right|$ are respectively the minimum and maximum acceptable corresponding line-to-line or line-to-neutral (depending on bus grounding) voltages magnitudes. Again this constraint must hold for all load levels.

The apparent power constraint is defined mathematically as:

$$P_i + jQ_i \le \left|S_i^{\max}\right| \quad \forall \quad i \in \textit{feeder / XFMR} \quad \forall \quad LL = 1 \cdots n_{LL} \tag{2.3.4}$$

i is a bus within the set of feeder or transformer. Since multi-phase switching will change the apparent power at the feeder and transformer this constraint must be valid for all load levels otherwise overloading of a transformer or feeder may occur. In this thesis ,individual feeders start at corresponding transformers. $S_i^{\max}$ is the maximum acceptable apparent power for the feeder or transformer.

The second type of inequality constraint for the multi-phase switching problem is to minimize the total level of imbalance among the in-service phases of bus i. The output of

the power flow, which is the state of the system, is utilized. The electrical parameters $\{|S|,|I|,|V|\}$ are examined for each in-service phase to determine the level of imbalance from the average.

This thesis selects from [1] the arithmetic mean or average as the target for performing network reconfiguration. Other methods include switching on the minimum value of a bus, and switching on the maximum value of a bus. The desired outcome from performing network reconfiguration is to transfer power or current downstream of a bus that exceeds the acceptable level of imbalance, such that the present phases at a bus equals the average electrical parameter $\{|S^{avg}|,|I^{avg}|,\text{or } |V^{avg}|\}$.

As a result of transferring current or power the voltage at other buses will be impacted. There are a limited number of switches in the network. The probability for electrical parameters to equal their average values at all phases is low. Hence a practical problem formulation is presented and the desired outcome for network reconfiguration has been relaxed to perform switch operations such that the phases of a bus are within a specified tolerance.

$$\left(\left|X_{i,LL}^{p}\right|-\left|X_{i,LL}^{q}\right|\right)\le imb\_tol_i \qquad \forall p,q \in \{A,B,C\} \qquad (2.3.5)$$

where:

imb_tol_i : *User defined tolerance at a bus i*

Therefore an unbalanced bus is defined as any bus comprising one or more phases that exceeds the phase difference and the user specified tolerance. Single phase buses are

considered to be balanced. In addition, phases of buses that are equal to zero are excluded from being checked for imbalance. Phases of buses that are equal to zero can be phases that are not energized (electrically connected) or phases that are not in existence. Single phase and two-phase lines are an example of buses with phases that are not in existence.

2.3.3 Network Constraints

A common practice of electric distribution companies is for the distribution system to remain in a radial configuration. A radial configuration is often necessary for coordination of protective devices. Maintaining a radial structure is required for the multi-phase switching problem. It is noted that this guideline exists in most papers [3, 12, 16, 24, and 28]. To observe and maintain a radial structure a sectionalizing switch must be opened first and then a corresponding tie-switch closed.

2.4 Overall Problem Formulation

The problem formulation is stated below in its entirety:

$$\min_{g_k} C_{pi}(n_{sw}^{n}(g_k^0, g_k)) + C_m(n_{sw}^{n}(g_k^0, g_k) + n_{sw}^{e}(g_k^0, g_k))$$

S.T.

$$F_{LL}(g_k) = 0 \qquad LL = 1 \cdots n_{LL}$$

$$\left|I_k\right| \le \left|I_k^{\max}\right| \qquad \forall \quad k \in \textit{all energized branches}$$

$$\left|V_i^{\min}\right| \le \left|V_i\right| \le \left|V_i^{\max}\right| \qquad \forall \quad i \in \textit{all energized buses}$$

$$P_i + jQ_i \le S_i^{\max} \qquad \forall \quad i \in \textit{feeder / XFMR buses}$$

$$\min_{g_k}\left(\left|V^{\phi Diff}\right|\right) = \left(\left|V_{i,LL}^{p}\right| - \left|V_{i,LL}^{q}\right|\right) \le imb\_tol_i \qquad \forall p,q \in \{A,B,C\}$$

$$\min_{g_k}\left(\left|I^{\phi Diff}\right|\right) = \left(\left|I_{k,LL}^{p}\right| - \left|I_{k,LL}^{q}\right|\right) \le imb\_tol_k \qquad \forall p,q \in \{A,B,C\}$$

$$\min_{g_k}\left(\left|S^{\phi Diff}\right|\right) = \left(\left|S_{i,LL}^{p}\right| - \left|S_{i,LL}^{q}\right|\right) \le imb\_tol_i \qquad \forall p,q \in \{A,B,C\}$$

One way of handling corresponding constraints is through the penalty function method. The scalar penalty function method applies a real number multiplier to each constraint of an optimization problem. The number acts as a weight for each equality and inequality constraint and assists in developing a metric for optimality. Then, a constrained problem is transformed to an unconstrained problem by adding the scaled constraints to the objective function.

These weights penalize an option by increasing the objective function value when a constraint is violated. For a minimum optimization problem the optimal solution will be the solution with minimal constraint violations and thus the lowest score.

2.5 Summary

Phase balancing may not be realized using existing control techniques. Existing control techniques may not necessarily reduce the imbalance caused by DER to an acceptable

level. Thus, network reconfiguration using multi-phase switches for phase balancing is proposed in this thesis.

In the next section, a switching scheme that minimizes the imbalance among the phases is developed. In addition, the switching scheme will minimize the costs of purchasing and installing new multi-phase switches and the costs for maintaining both new and existing switches. Phase balancing is needed if and only if the initial power flow configuration violates acceptable levels of system imbalance. The next chapter presents the solution algorithm for the multi-phase switching problem.

Chapter 3. Solution Algorithm

The solution algorithm for multi-phase switching for phase balancing in radial distribution systems is presented in this chapter. This solution algorithm relies on a heuristic method to perform network reconfiguration for a bus that has been identified to have an unacceptable level of imbalance. The algorithm which depends on analytically determined network indices is presented.

3.1 Procedure

The main steps for the solution algorithm are:

Step 1. Run unbalanced power flow

Step 2. Determine the level of imbalance at all buses for parameters |*S*|, |*I*|, and |*V*|,

Step 3. Find the list of unbalanced buses and phases to create an unbalanced node list

Step 4. Rank the list of unbalanced nodes

Step 5. Select a new set of open and closed switch operations (g_k) to be performed

Step 6. Repeat Steps 1 – 5 until all lists are within tolerance or stopping criterion is reached

In the following subsections the six steps outlined above are discussed. Necessary alterations made to a common power flow solver data format and data structures are described first. Then, a measure of the acceptable level of imbalance from the average at

a bus is presented. This metric is the basis for determining the unbalanced node lists. Section 3.4 illustrates this process and discusses the target value for switching. Section 3.5 describes the process for finding the unbalanced buses and phases to create the unbalanced node lists. Section 3.6 explains a ranking scheme for the resultant unbalanced node lists. Section 3.7 discusses the procedure for selecting a set of switch operations to reduce the imbalance at a bus. Section 3.8 explains the acceptance criterion for proposed switch operations. Section 3.9 explains penalty costs for constraint violations. Section 3.10 reviews instances in which buses are permitted to remain unbalanced. Finally, the last section illustrates ordering and sorting the unbalanced node lists for parameter $|S|$ and a user specified tolerance of 2%.

3.2 Unbalanced Component Models and Power Flow Solver

Adapted from [29], Figure 3.1 below shows the types of injections that exist in the distribution system. This figure has been altered to include PHV generators.

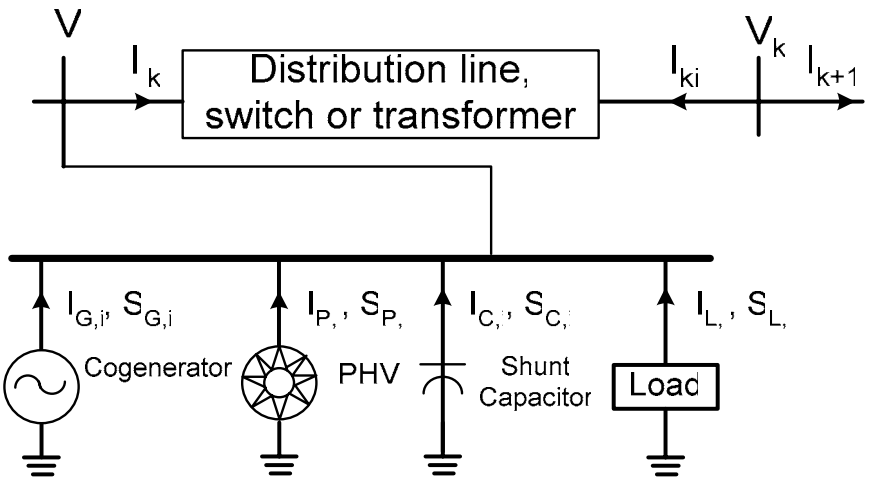

Figure 3.1 Basic building block of a distribution system, revised to include PHV generators

Figure 3.1 is a two bus system, with buses i and k. Four components are injecting current and power into bus i. The components are a cogenerator, PHV, shunt capacitor, and load. There exists a distribution switch, line, or transformer connecting bus i and bus k to form branch ik. The network continues from bus k to a new bus, $k+1$, which is not shown in the figure but whose branch current is identified as $I_{k,k+1}$.

Distribution components can be single or multi-phase. Mutli-phase includes all two-phase combinations (i.e. *AB*, *BC*, *CA*) and three phase combinations (*ABC*). In this thesis, all parameters in Figure 3.1 are steady state variables and are defined as:

V_i : *Voltage at bus i*
V_k : *Voltage at bus k*
I_{ik} : *Current across branch i to k*
I_{ki} : *Current across branch i to k*
$I_{k,k+1}$: *Current across branch k to* $k+1$
$I_{L,i}$: *Current injection into bus i for a load L*
$S_{L,i}$: *Apparent Power injection into bus i for a load L*
$I_{(C,P,G),i}$: *Current injection into bus i for a* (*Capacitor*, *PHV*, *or Cogenerator*)
$S_{(C,P,G),i}$: *Apparent Power injection into bus i for a* (*Capacitor*, *PHV*, *or Cogenerator*)
L : *Load bus*
C : *Capacitor*
P : *PHV*
G : *Cogenerator*

The variables above are represented as (*3 x 1*) complex vectors, and contain zeros for phases that are not present.

A nodal power flow solver is needed to represent the unbalanced parameters in Figure 3.1. In [31] a power flow program was written utilizing bus-oriented data structures. Significant changes to the data structures utilized in [31] were necessary in order to complete step one of the procedure. In order to run an unbalanced power flow, the data formats and the data structures were changed. The changes to the existing bus structured power flow program are presented in the next subsection of this chapter.

3.2.1 Data Format Changes for Unbalanced Power Flow Solvers

The power flow solver used in this investigation required the network data to be entered using PTI – PSSE version 7 format from [32] and is later referred to as the standard power flow format. The power flow bus structure from [31] was altered to a nodal structure. A node corresponds to a bus and a phase. The nodal structure allows for one incoming branch per phase of a bus and one outgoing branch per phase of a bus.

The connection status of a branch originally was represented in PTI – PSSE version 7 as either a "1" for in-service buses or "0" for out of service buses. The connection status data format was changed to include the service status of each phase of a bus. The new connection status format has a "1" or a "0" for each phase of a branch. Both the connection status data format and data structure were altered. In the next subsection the changes to the data structures are discussed.

3.2.2 Data Structure Changes to Power Flow Solver

The switches that were implemented in [31] were three phase switches. Disconnecting and connecting the individual phases of the switch was not possible in the original bus data format model structure. A single-phase or two-phase switch would have to be modeled separately. The network switches are now modeled on per phase or nodal basis. A multi-phase switch can be configured to operate as a three-phase, two-phase or single-phase switch.

Specifically, the connection status data structure from [31] was changed to reflect the change in the data format. The size of the connection status data structure was increased from a (*1 x 1*) vector, to a (*1 x 3*) vector with ones and zeros.

	PTI – PSSE version 7	**New Connection Status**		
	Phase ABC	**Phase A**	**Phase B**	**Phase C**
Branch 5	[1]	[1	1	0]

e.g. Comparison of PTI-PSSE version 7 and New Data Structure for Branch 5

Previously a branch could be represented by only having all three phases connected (1) or disconnected (0), now two phases may be connected and disconnected. Also, the original data structure relied on buses to associate data. Thus, in a radial network, the connectivity would allow only one incoming branch per bus and one outgoing branch per bus. Figure 3.2 below is an example of network connectivity using the original power flow.

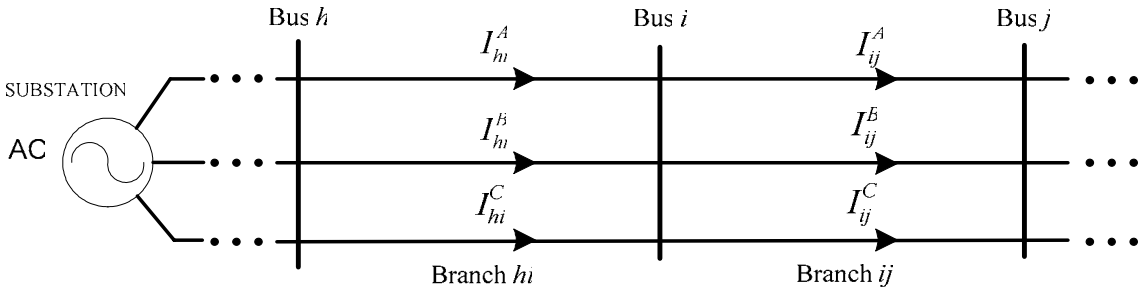

Figure 3.2 Original Network Connectivity

The network in Figure 3.2 shows a three-phase and three bus system. There is a substation serving three phase power to buses h, i, and j. The current flows from the substation though branch hi and branch ij. Bus i is a three phase bus with phases

A, B, and C from bus h and phases A, B, and C going to bus j. In this model each bus and associated phases is allowed one "to" bus and one "from" bus. This network connectivity was changed from a bus structure to a nodal structure. The revised connectivity is shown in Figure 3.3.

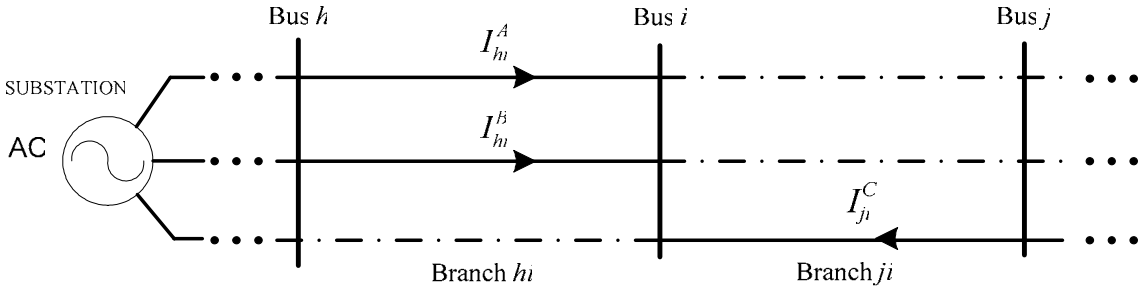

Figure 3.3 Revised Network Connectivity

The revised power flow structure illustrated above in Figure 3.3 is an example of the nodal structure. There is a substation serving three phase power to buses h, i, and j. The current flows from the substation though branch hi for phases A and B. The current flows from the substation through branch ji for phase C. The dashed-dot lines in Figure 3.3 above indicate that a phase is present at a branch but is not electrically connected (e.g. a switch). Bus h is a three-phase bus with two-phases present, phases A and B. Bus i is a three phase bus with phases A, B, and C. Bus j is a three-phase bus with one-phase present, phase C. It is noted that the path to the substation is different for phase C in comparison to phase A and B and in comparison to Figure 3.2. The voltage drop from each path to the substation is unique. However, voltage constraints and $imbal\_tol_i$ prevent a very large difference in voltage drop across the phases at a bus i. In the new

model each node can have its own “from” bus and “to” bus. Thus the data structure size is increased to $n_{buses} \times 3$.

In order for the single-phase and two-phase switches to operate in a nodal manner, the branch data structure was changed. Previously, the data format and consequently power flow solver relied on a static scalar parameter describing the connected phases of a branch. The branch data structure now identifies physical connections of each phase of a branch using a (*1 x 3*) vector in order to represent changes in individual phase connection statuses. Additional adaptation to the program was performed and list details can be found in the appendix.

Changes to the switching method were made possible by the shifting in the power flow structure from a bus to a nodal structure. In the next subsection the impacts from the nodal power flow structure are discussed. Specifically, nodal switch modeling capabilities is described.

3.3 Determining the Level of Imbalance at all Buses

The level of imbalance was quantified in Chapter 2. The average of the present phases at a bus and the phase differences at a bus are needed to determine the level of imbalance.
In Chapter 2 the phase difference was defined in eqn. 2.1.5 and is repeated below. Throughout this section the terminology phase difference or phase-to-phase will represent:

$$\left|X_{i,LL}^{p,q}\right| = \left|X_{i,LL}^{p}\right| - \left|X_{i,LL}^{q}\right| \qquad (3.3.1)$$

This definition is necessary to distinguish between line-to-line notations, which are often referred to as phase-to-phase. In addition, all electrical parameters |*S*|, |*I*|, |*V*|, and θ_V are phase-to-phase expressions at a bus. The difference is that the current and power values are not found by measuring across a branch, they are found by measuring across the present phases at a bus.

The arithmetic mean or average was selected as the target for performing network reconfiguration. Other targets include switching on the minimum value of a bus, and switching on the maximum value of a bus. A comparison of the three methods is presented next.

The technique for finding the list of unbalanced nodes, Step 3, is described in the next section.

3.4 Finding the List of Unbalanced Nodes

The lists of unbalanced nodes are determined in two parts. Recall that a node consists of a bus and a phase. First, the unbalanced buses are identified from the phases at a bus that exceed an acceptable level of imbalance. Secondly, the unbalanced phase is determined from finding the phase difference that is the maximum difference from the average parameter. Parameters include $|S|$, $|I|$, and $|V|$. The structure of the unbalanced node list is $Unbalanced\ node = \left[bus,\ \Phi\left(\left| X_{i,LL}^{\max diff} \right| \right) \right]$.

The steps for determining the unbalanced node lists are:

1. Compute phase difference: $\left|X_{i,LL}^{p,q}\right| = \left|X_{i,LL}^{p}\right| - \left|X_{i,LL}^{q}\right|$

2. Compute average for present phases: $\left|X_{i}^{avg}\right| = \dfrac{\sum_{p=1}^{n_{ph}} \left|X_{i}^{p}\right|}{n_{ph}}$

3. Compute maximum phase difference from the average:

   $\left|X_{i,LL}^{\max diff}\right| = \max_{p=1\ldots n_{ph}} \left(\left|X_{i,LL}^{avg}\right| - \left|X_{i,LL}^{p,q}\right|\right)$

4. Measure imbalance from average: $\left(1 - \dfrac{\left|X_{i,LL}^{avg}\right| - \left|X_{i,LL}^{\max diff}\right|}{\left|X_{i,LL}^{avg}\right|}\right) \times 100 = \%\ Imbalance$

5. Check $\%\ imbalance \le imb\_tol_i,\ \ for\ \ |S|,\ |I|\ \ and\ \ |V|,$

6. if any violations are identified then record the unbalanced node and corresponding bus

3.4.1 Determining Unbalanced Buses

An unbalanced bus was defined in the problem formulation as any bus comprising one or more phases that exceeds the phase difference and the user specified tolerance. In general, the procedure is to find all buses:

$$\left|X_{i,LL}^{p}\right| - \left|X_{i,LL}^{q}\right| \le imb\_tol_i \qquad \forall p,q \in \{A,B,C\} \qquad (3.4.1)$$

For example, an acceptable phase difference between two phases for |*V*| is an absolute value of 5% as per [1]. This concept also applies to the apparent power, and current magnitude.

3.4.2 Determining Unbalanced Phases

From the list of unbalanced buses the phase difference that is the maximum from the average is chosen as the unbalanced phase for a bus. The maximum from the average was defined in the Problem Formulation and is repeated below:

$$\left|X_{i,LL}^{\max diff}\right| = \max_{p=1\ldots n}\left(\left|X_{i,LL}^{avg}\right| - \left|X_{i,LL}^{p,q}\right|\right) \qquad (3.4.2)$$

If two phase differences at a bus are equal then the first phase difference is taken as the unbalanced phase for a bus. The unbalanced node lists have been established.

3.4.3 Ordering Unbalanced Node Lists

The electrical parameters, $|S|$, $|I|$, and $|V|$ are grouped into separate lists which will be subsequently ordered and ranked. These lists form the unbalanced node lists. The priority of the ordering will now be discussed.

PHVs are considered to be the source of imbalance in the network. PHVs are modeled as an PQ injection into a bus. Since the converter maintains an often nearly constant power factor the imbalance predominately stems from the real power output, P, of a PHV. Thus $|S|$ was chosen as the first electrical parameter to examine.

Furthermore, since power flows directly link to current flows $|I|$ was chosen as the second parameter to balance. It is assumed that if a node's imbalance is due to $|S|$ then its

level of imbalance will be similar for $|I|$. It is believed by reducing the level of imbalance at $|S|$ the level of imbalance at $|I|$ will decrease proportionally. Thus it may be possible to correct the level of imbalance for both $|S|$ and $|I|$ with the same network switching scheme. Further unbalanced flows result in imbalance due to V thus $|V|$ is examined third. The lists are referred to as the unbalanced node lists. In the following section Step 4, the unbalanced node lists are ranked in order of importance.

3.5 Ranking the List of Unbalanced Nodes

An unbalanced node and bus is classified by two categories, the location of imbalance and the size of the imbalance. This solution algorithm primarily relies on the location of the buses to achieve a phase balanced network. The size of imbalance is implemented when two unbalanced nodes have buses that are equal distance from a transformer. In this thesis the transformers are also the feeder buses in the network.

In a radial network, upstream refers to the direction of current defined with respect to the substation. Pairs are defined as adjacent unbalanced buses. Pairs indicate that an area is unbalanced. It is desired to balance areas first because it is possible to impact and improve multiple buses.

For a particular bus, there are two possible instances for buses upstream to be unbalanced. First, there could be a single or pair of unbalanced buses affecting multiple buses upstream. Second, there may be a single or pair of unbalanced buses affecting a

single bus upstream. It is believed that fixing the furthest bus downstream will effectively impact the unbalanced buses upstream and may reduce the imbalance to an acceptable level. Below is an overview of the ranking of unbalanced node lists:

Unbalance node lists are first ranked by:

1. Location from transformers/feeder buses
2. Size of imbalance

The ranked unbalanced node lists are separated into:

1. Pairs of unbalanced buses
2. Single unbalanced buses

The pairs and single unbalanced node lists are subsequently ranked by:

1. Industrial customer(s)
2. Unbalanced buses located downstream of industrial customer(s)
3. Farthest downstream unbalanced node and corresponding bus

Network Reconfiguration is then performed on the lists in order of:

1. Ranked unbalanced pair's node list
2. Ranked unbalanced single's node list

The current unbalanced node and corresponding bus are defined as the first entry in the ranked unbalanced pair's node list. Once all of the unbalanced node pairs have been examined for network reconfiguration the program proceeds to the ranked unbalanced single's node list. Details on this implementation can be found in the following subsections.

3.5.1 Ranking Unbalanced Nodes Lists by Location

The bus triple variable from [30] is employed for finding the location of buses for the unbalanced nodes. The bus triple variable is an indexing scheme created to track the order in which the network was traversed using the reverse breadth-first (RBF) search method. It consists of three different pointers per bus (l, m, n). The first pointer l, is the level of the lateral. This represents the number of laterals for a level which will be traversed, counting from the end of the lateral to the source. The second pointer m, is the lateral index within a lateral. m is the index according to the order seen during the RBF search method. The last index n, is the bus index within a lateral.

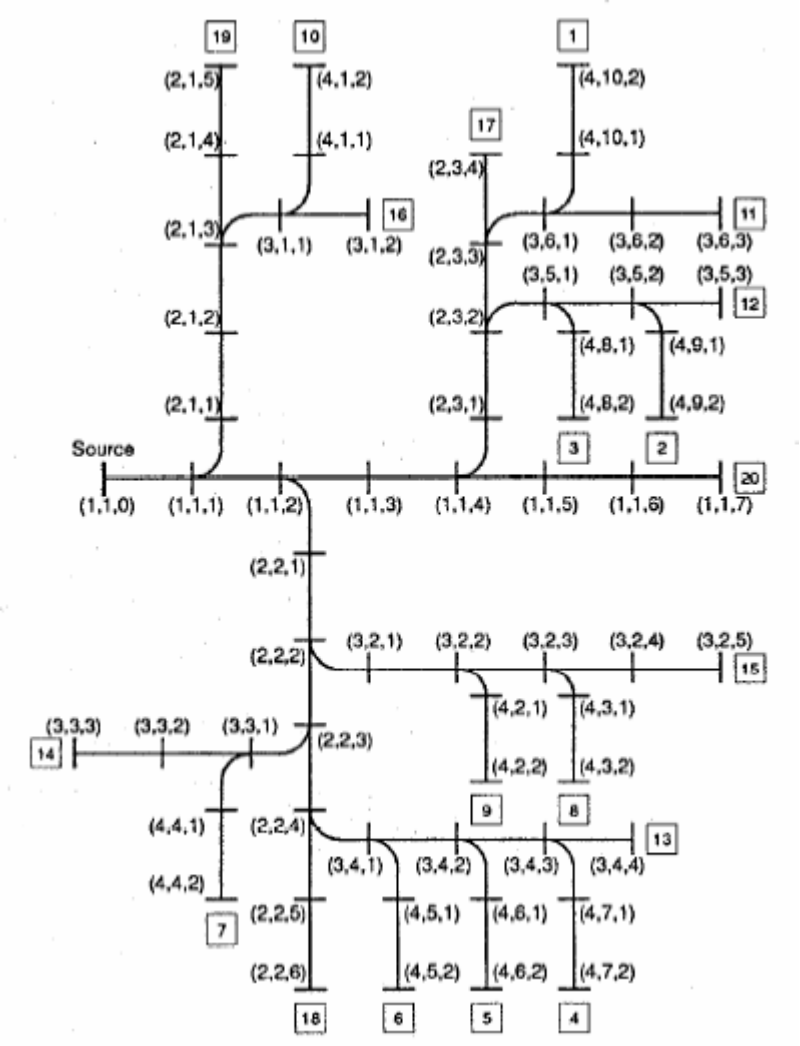

Figure 3.4 Example of 63-Bus System, Bus and Lateral Indexing from [30]

Above, in Figure 3.4 the boxed numbers show the RBF ordering of the laterals found by sorting the lateral indices in reverse order, first by level, then by lateral index. The bus triple is read as the n^{th} bus on the m^{th} lateral on the l^{th} level. [30]. For example, (2,2,1) in Figure 3.4 above is read as the first bus on the second lateral and second level. The unbalanced node lists are ranked by utilizing the bus triple variable to order the buses in decreasing distance from the transformers.

3.5.2 Ranking Unbalanced Node Lists by Size

The second category of ranking, the size of imbalance is used to determine the order of the nodes that are on different laterals but have buses with equal distances from a transformer. The equi-distance lateral gives cause to sort the nodes with equal distances by their size. They are arranged in order of their size from the largest level of imbalance to the smallest level of imbalance. This new order with respect to size is applied to the unbalanced node lists by overwriting the rank of their previous entries. Post ranking, the unbalanced node lists are sectioned into unbalanced node pairs and single unbalanced nodes.

3.5.3 Creating Unbalanced Node Pairs

As stated previously, pairs indicated an area of unbalanced buses. It is advantageous to balance an area in comparison to single unbalanced nodes because it is possible to impact and improve multiple buses. All unbalanced nodes that have buses on the same level and lateral are examined to create a list of unbalanced node pairs. An unbalanced node pair is any two nodes that have buses that are on the same level and lateral and whose bus indices are consecutive.

A forward sweep is performed on unbalanced node lists to find pairs of unbalanced to-buses. The node pair list maintains the order established in subsection 3.6.1.

A second list is subsequently compiled of single unbalanced to-buses. This is accomplished by performing a second forward sweep and removing all node pairs. The single unbalanced node list also preserves the order established in subsection 3.6.1.

All equi-distance lateral conflicts for the unbalanced node lists were resolved previously by arranging the buses by size as explained in subsection 3.6.2. If the resultant unbalanced node lists consist of one unbalanced node the method for balancing is simplified. The method for balancing consists of searching for switches downstream to balance the phases at the specific node. However, if two or more unbalanced nodes exist then the nodes are ordered according to priority customers.

3.5.4 Ordering Unbalanced Node Lists by Customer

Priority customers are predominately industrial customers, hospitals, banks and large commercial customers. This thesis selects the industrial customer as the priority customer. Thus the unbalanced node pairs and single node lists are ranked giving priority to:

1. Industrial customer(s)
2. Unbalanced nodes downstream from industrial customers
3. Farthest downstream unbalanced node and corresponding bus

The nodes closest to the industrial customer are believed to help correct the imbalance at the industrial customer. The farthest downstream node is believed to impact and may improve the level of imbalance at upstream nodes.

Again, the current unbalanced node is defined as the first entry in the ranked unbalanced node lists. Knowledge of the power system is used to perform a forward search beginning with the first node on the ranked list to search for tie-switches downstream that could reduce the level of imbalance. The process of finding tie-switches to reduce the imbalance to an acceptable level for the parameters |*S*|, |*I*|, and |*V*|, is described in detail in Step 5, selecting a new set of open and closed switch operations.

3.6 Selecting a New Set of Switch Operations (g_k)

Sorting and selecting a new set of switch operations, (g_k), is driven by the constraints outlined in Chapter 2. Recall from chapter 1 that a sectionalizing switch is a switch that is normally closed and a tie switch is a switch that is normally open. Throughout this section, sectionalizing switches are referred to as *SS*, or normally closed switches. Tie switches are referred to as *TS*, or normally open switches.

A switch operation is defined as the act of opening or closing a sectionalizing or tie-switch. A switch pair consists of two switch operations. The first operation is the opening of a sectionalizing switch and the second operation is the closing of a matching tie switch. As discussed in Chapter 2 this ensures that a radial structure is maintained. A matching tie switch is a normally open switch that will restore power to buses once the sectionalizing switch has been opened.

It is desired to find a *TS*-*SS* pair such that no current or power at a branch will become overloaded. These were represented as constraints in the problem formulation chapter (eqn. 2.3.2 -2.3.4). In addition, it is preferred to find a *SS* such that the level of imbalance at all nodes upstream from the *TS* is not increased. The switching algorithm uses several heuristics to determine switch operations that will prevent violating electrical and thermal constraints and prevent from increasing the level of imbalance at upstream buses. These heuristics include utilizing network indices: transfer current I^{SS} from [17] and spare capacity of a branch I^{m} from [16].

The transfer current for each phase of the switch is equal to the estimated amount of current that will be shifted by opening a sectionalizing switch.

$$\left|I^{SS}\right| = \left|I_{ik}\right| \qquad (3.6.1)$$

The spare capacity of a branch was defined as:

$$I^{m} = I^{p}_{rating} - I^{p}_{p.u.} \qquad (3.6.2)$$

I^{p}_{rating} is the rating of each phase of the switch in per unit. $I^{p}_{p.u.}$ is the per unit current flowing through the branch up to the tie-switch. I^{m} is the margin or spare capacity on a feeder per phase. The spare capacity of transformer was found by converting the transformer KVA into a per unit current rating.

The minimum spare capacity along the path from a *TS* to the substation is used in this thesis to ensure that switch pairs are selected such that no current or power at a branch will become overloaded and was re-defined at each phase of branch.

In [17], switch ranking indices were developed to restore load to priority customers in the least amount of time while observing electrical, thermal, and operational constraints. Among these indices are the spare capacity of a branch, I^m, and the transferable load (transfer current), I^{SS}. For example, I^{SS} is the maximum current flow through the phases of a sectionalizing switch which is opened to transfer load. In this thesis I^{SS} was re-defined as the current flow through each phase of a branch.

The algorithm for selecting a set of switch operations for the current unbalanced node is:

1. Find and store the index of all downstream TS and SS
2. Find the spare capacity (I^m) of the downstream switches
3. Find the transfer current (I^{SS}) for the current unbalanced node
4. Rank the switches in descending order by I^m
5. Find and rank *TS-SS* pairs using works [16 and 17]
6. Check $I^{SS} < I^m_{imbal}$, where I^m_{imbal} is the spare imbalance
7. Select switch pairs for phase balancing

In the subsections below, details for selecting a new set of switch operations (g_k) can be found.

3.6.1 Finding and Storing Switch Indices

The first step towards selecting a new g_k is to use a forward search on the current unbalanced node to find and store the index to all tie and sectionalizing switches that are downstream. Recall from the problem formulation chapter that:

$$g_k = \left[g_k^A, g_k^B, g_k^C \right] : \textit{set of sectionalizing and tie switches} \quad (3.6.3)$$

After the indices to the downstream *SS* and *TS* have been ascertained the transfer current (I^{SS}) and spare capacity (I^m) for each phase of the switches are measured.

3.6.2 Ordering Switches by Transfer Current (I^{SS}) and Spare Capacity (I^m)

The list of tie-switches is organized in descending order by I^m. The switches with the greatest spare capacities are examined first because it is easier to transfer current to and from them in comparison to a switch with a smaller current capacity.

The number of possible TS-SS pairs is limited by the amount of I^m and amount of I^{SS} that is available at a branch. Electrical and thermal violations would occur if the amount of current that was transferred to a switch was greater than the available spare capacity at a switch. Therefore transferring $I^{SS} > I^m$ is prohibited. The next step in selecting a new g_k is to utilize the above heuristics to find all possible tie-switch (*TS*) and sectionalizing switch (*SS*) pairs.

3.6.3 Finding TS and SS Pairs

In order to find switch pairs a forward and backward search on the list of TS for the current unbalanced node is performed to find all possible SS. The search starts with the farthest downstream *TS* and proceeds until the flagged sectionalizing switch is found. The flagged sectionalizing switch is the switch that will be opened to reduce the level of imbalance at the current unbalanced node. If the search encounters a substation or feeder bus before finding the flagged sectionalizing switch then no *TS-SS* pair exists for the current unbalanced node. The program would return to the unbalanced node lists and continue to find all SS-TS pairs of the remaining nodes.

If a *TS-SS* pair is found its location is stored. The program continues to search for other *TS-SS* pairs until a substation is reached. After all pairs are found the *TS* spare capacity is checked to guarantee that $\left|I_{ik}^{m}\right| \le \min\left|I^{m}\right|$. If the $\left|I_{ik}^{m}\right|$ is not less than the minimum $\left|I^{m}\right|$ of all of the branches then the tie switch does not make an eligible switch pair and its index is discarded.

For all eligible tie switches the current at the branch is checked to ensure that $\left|I_{ik} - I_{ik}^{avg}\right| \le \left|I_{ik}^{avg}\right|$. The switch with the smallest $\left|I_{ik} - I_{ik}^{avg}\right|$ is the switch whose size is closest to the average. The sectionalizing switches are ranked in descending order of $\left|I_{ik} - I_{ik}^{avg}\right|$. If $\left|I_{ik} - I_{ik}^{avg}\right|$ is greater than $\left|I_{ik}^{avg}\right|$ the TS-SS pair is removed because the TS will transfer more than the average. Transferring more current then the average would cause an increase in imbalance at that node.

Thus the following constraint is included.

$$I^{SS} < I^{m}_{imbal} \qquad (3.6.4)$$

where:

$$I^{m}_{imbal} = I^{tol\_i} - \left| I^{\phi Diff} \right|$$

$$I^{tol\_i} = I^{avg} * imbal\_tol_k$$

$$\min_{g_k}\left(\left| I^{\phi Diff} \right|\right) = \left(\left| I^{p}_{k,LL} \right| - \left| I^{q}_{k,LL} \right|\right) \le imb\_tol_k \qquad \forall p,q \in \{A,B,C\}$$

I^{m}_{imbal} is the spare imbalance of the *TS's* branch. Checking the available difference between the spare imbalance and I^{SS} ensures that current will not be transferred such that the level of imbalance will increase at buses upstream of the *TS*. Therefore, if I^{SS} is greater than the available spare imbalance the switch pair is discarded.

Switch operations for eligible switch pairs are performed according to the above rank. Post switching the accepting or stopping criterion for the set of g_k is checked. The accepting criterion is described in the next section.

3.7 Accepting Criterion

An overview for accepting criterion for g_k follows:

1. Convergence of power flow solver with new set of switch statuses
2. Electrical and thermal constraints cannot be violated
3. Level of system imbalance and unbalanced node's imbalance cannot increase
4. $n^{n}_{op} - n^{n-1}_{op} < 0$ and $n^{0}_{op} = 2$

where:

5. n_{op}^{n} : *number of switch operations for current iteration*
   n_{op}^{n-1} : *number of switch operations for previous iteration*

6. Downstream buses remain unbalanced

7. If $N_{non} = N_{non}^{\max}$ then stop

where:

8. N_{non} : *number of non-improving moves*
   $N_{non}^{\max}$: *maximum number of non-improving moves*

The details for the accepting criterion are discussed in the subsections below.

3.7.1 Power Flow and Constraint Checking

Run power flow solver with the new set of switch statuses to ensure that the solution will be feasible. If the power flow solver doesn't converge then the next set of switch pairs is selected.

Upon convergence the results are post processed and all inequality constraints are checked for violations. Again the phase difference for each node's bus is computed and checked to be within the user specified tolerance.

3.7.2 Determine Unbalance Nodes at New g_k

The number of unbalanced nodes is determined. If the number of unbalanced nodes increases then the set of switch operations is rejected. In addition if the severity of

imbalance at a node's bus increases, in other words if, $\left|I_{ik}\left(g_k\right)-I_{ik}\left(g_k{}^{n-1}\right)\right|>\left|I_{ik}\left(g_k{}^{n-1}\right)\right|$ then the set of switch operations is discarded. Here, $I_{ik}\left(g_k\right)$ is the current from bus i to bus k for the current set switch statuses. $I_{ik}\left(g_k{}^{n-1}\right)$ is the current from bus i to bus k for the previous set of switch statuses.

3.7.3 Number of Switch Pairs

Post convergence the number of switch pairs is counted.

$$If\ \ n_{op}^{n}-n_{op}^{n-1}<0\ \ then\ continue \tag{3.7.1}$$

Above n_{op}^{n} is the number of switch operations for the current iteration, and n_{op}^{n-1} is the number of switch operations of the previous iteration. The n_{op}^{n-1} is set to equal 2 for the g_k^0. Otherwise, the program would not accept g_k because g_k^0 having $n_{op}=0$ would be the most desirable case. An increase in the number of operations is undesirable because this violates the objective stated in the problem formulation to minimize the number of switch operations. In addition, this is undesirable because the life of the switch is reduced each time a switch is operated. Consequently, maintenance will have to be performed earlier then scheduled routine repairs. If the number of switch operations increases then $g_k^n=g_k^{n-1}$. The number of non-improving moves N_{non} is incremented and the program terminates if $N_{non}=N_{non}^{\max}$. $N_{non}^{\max}$ is the maximum number of non-improving moves.

3.8 Penalty Cost for Constraint Violations

The solution to the multi-phase switching problem is based on the cost for performing network reconfiguration. From all possible g_k the set of switches that produces the least cost is selected. As stated in the problem formulation the penalty method is used to assign costs for constraint violations.

The switch pairs that are rejected receive a penalty cost. The penalty costs assigned to switching violations are listed below in order of largest to smallest penalty:

1. $\left|I_{ik} - I_{ik}^{unbal}\right| > \left|I_{ik}^{unbal}\right|$
2. $n_{op}^{n} - n_{op}^{n-1} > n_{op}^{n-1}$
3. Downstream nodes remain unbalanced

The final penalty cost which has the lowest cost associated is for downstream nodes to remain unbalanced. The instances in which nodes downstream are permitted to remain unbalanced are explained in the next chapter section.

3.9 Situations Where the Current Downstream is Permitted to be Unbalanced

The current downstream is permitted to be unbalanced for two different conditions. The first condition is if by balancing the current at a downstream node causes the upstream node to become unbalanced. This includes but is not limited to an industrial customer or

transformer bus becomes unbalanced as a result of reducing the imbalance to an acceptable level for a downstream node. The second condition is if switching will cause the resultant current to be greater than the spare capacity (I^m) available at a branch.

This decision process has been coded in the solution algorithm. The heuristics above are pertinent in finding a solution because they reduce the size of the problem by eliminating nodes and they provide guidelines for accepting switch operations. Both conditions for the system to remain unbalanced are equally important and violating either or both will result in changing the parameter $\{|S|,|I|,|V|\}$ to balance.

3.10 Example of Ordering and Sorting Unbalanced Nodes for a 9-Bus Case

An example system that used to illustrate the solution algorithm is 12-bus system. The electrical parameter |*S*| was selected to be examined and the imbalance tolerance was chosen to be 2%. Figure 3.5 below is a diagram of the system.

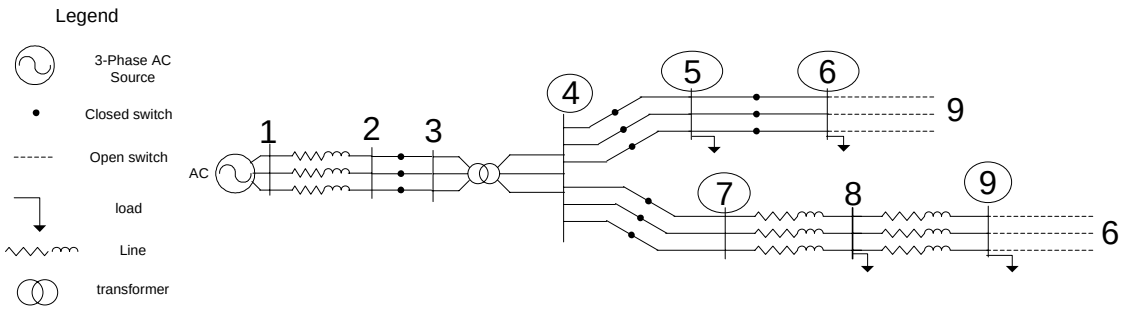

Figure 3.5 Example of 9-Bus Case

In Figure 3.5 there is a substation with three-phase power and a three-phase transformer. A total of five switches exist, of which two are tie-switches and three are sectionalizing

switches. There a total of four loads in the 9-bus case. Buses 4, *5, 6, 7*, and *9* which are circled were found to be imbalanced for parameter $|S|$. The industrial customer in this example is located at bus 5. The unbalanced nodes and |*S*| percent imbalance are listed in Table 3.1.

Table 3.1 |S| % Imbalance for Unbalanced Nodes in 9-Bus Case

Unbalanced Node		
Bus	**Phase**	**S % Imbalance**
4	**A**	**3 %**
5	**A**	**5 %**
6	**A**	**7 %**
7	**A**	**3%**
9	**A**	**4 %**

The unbalanced nodes are ranked in decreasing order from the transformers using the RBF technique. The RBF index for each unbalanced node is listed in

Table 3.2 Reverse Breadth First Search Index for Unbalanced Nodes

Unbalanced Node			
Bus	**Phase**	**RBF index**	**Rank**
4	**A**	**[1,1,4]**	**4**
5	**A**	**[1,2,1]**	**3**
6	**A**	**[1,2,2]**	**2**
7	**A**	**[1,1,5]**	**3**
9	**A**	**[1,1,6]**	**1**

In Table 3.2 above, the unbalanced nodes *5* and *7* are equal distance from the transformer. These nodes are now ranked according to the size of imbalance using the |*S*|

percent imbalance listed in Table 3.1 and the previous rank is over-written with the new rank. The ranked unbalanced node list is shown in Table 3.3.

Table 3.3 Rank Unbalanced Node List

Unbalanced Node				
Bus	**Phase**	**RBF index**	**S % Imbalance**	**Rank**
4	**A**	**[1,1,4]**	**3 %**	**5**
5	**A**	**[1,2,1]**	**5 %**	**3**
6	**A**	**[1,2,2]**	**7 %**	**2**
7	**A**	**[1,1,5]**	**3%**	**4**
9	**A**	**[1,1,6]**	**4 %**	**1**

In Table 3.3 the order of the unbalanced node list is shown in column four. The RBF index and $|S|$ % imbalance are listed respectively in columns two and three. Now that list has been ordered the ranked unbalanced node lists are separated into pairs of unbalanced buses and single unbalanced buses. The pairs of unbalanced buses are shown in Table 3.4.

Table 3.4 Unbalance Bus Pairs

Unbalanced Pairs	
Bus	**Bus**
6	**5**
4	**5**
4	**7**

Three pairs of unbalanced buses were found in the 9-bus case. One single unbalanced bus in the 9-bus case exists and is bus 9. The industrial customer in this example is located at bus 5. The unbalanced pairs are ordered by section 3.4. and the order is listed below in Table 3.5.

Table 3.5 Order of Unbalanced Pairs

Unbalanced Pair		
Bus	**Bus**	**Order**
6	**5**	**1**
4	**5**	**2**
4	**7**	**3**

Network Reconfiguration is now performed on the unbalance pairs in order shown in Table 3.5 and subsequently the single unbalanced bus, bus 9. In the next section, the summary for this chapter is provided.

3.11 Summary

This solution algorithm that was presented in the chapter was a heuristic based algorithm. Several heuristics are outlined in this chapter. The heuristics was based on works [16] and [17] and included finding transfer current I^{SS} and spare capacity I^{m} of a branch.

The main steps of the algorithm that were discussed are:

- Running the unbalanced power flow
- Finding the average across the present phases at the buses for the parameters $\{|S|,|I|,|V|\}$
- Determining and ranking the list of unbalanced nodes
- Selecting a new set of switch operations to be performed

A flow chart outlining the algorithm is shown in Figure 3.6.

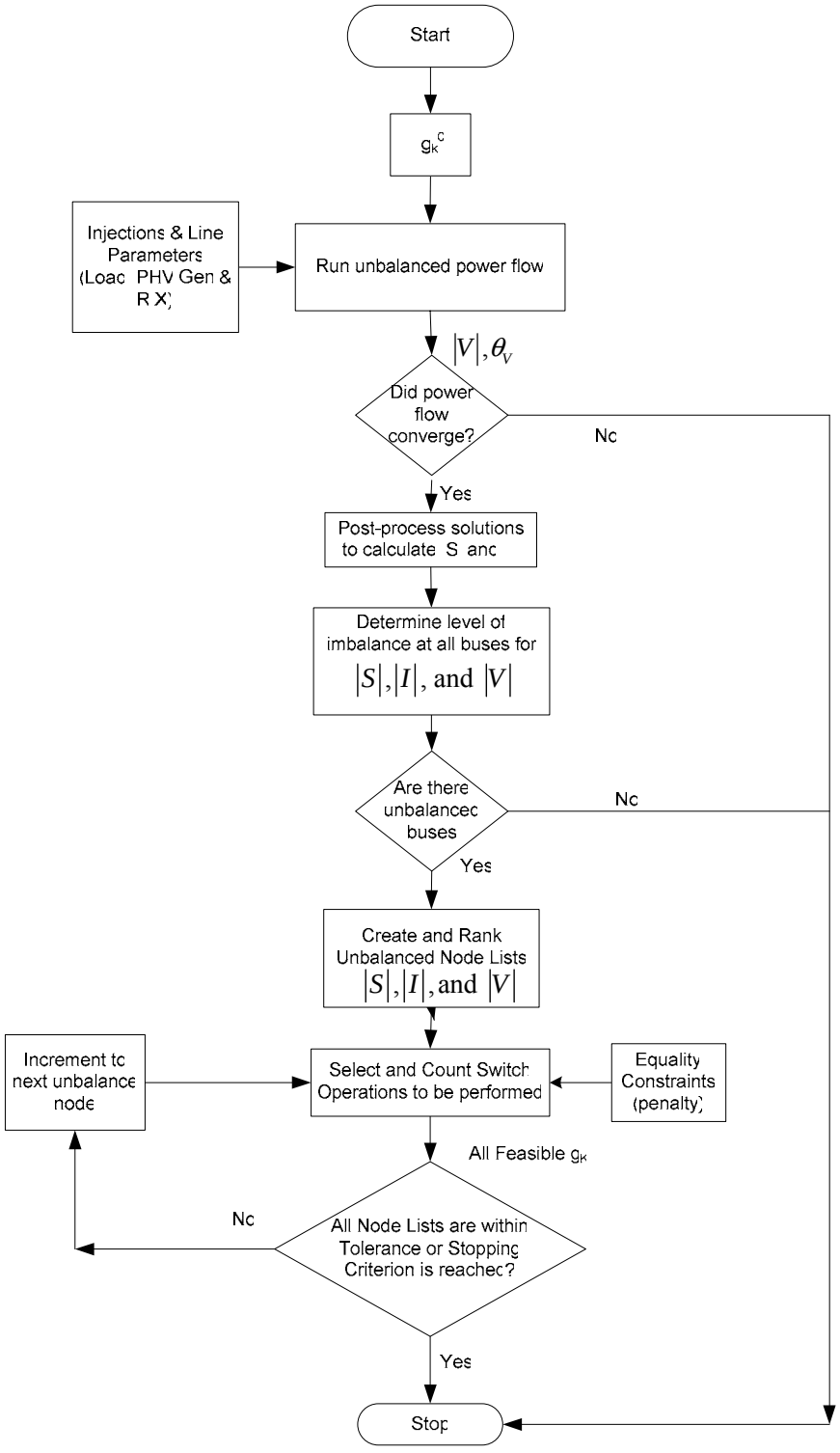

Figure 3.6 Flow Chart of Main Steps of Multi-Phase Switching Algorithm

In the next chapter, an example and the simulation results will be discussed.

Chapter 4. Simulation Results

In this chapter, the simulation results for the multi-phase switching algorithm are presented. In the following subsections the simulation set –up, case example, results and observations are given. It is noted that, from a system viewpoint, single-phase PHV installations in a practical case would be randomly placed because electric distribution companies do not control the installation location.

This is a reasonable assumption because in distribution system each street can be a different phase of one feeder. One phase of a feeder could connect to houses with a lot of southern exposure where as another phase of a feeder may not be facing south. Thus it is reasonable to assume that individuals with southern facing homes would install PHVs on their houses in comparison to those that do not have significant amounts of southern exposure. Thus, the feeder as a result of PHV installations would experience an imbalance among its phases.

The details of the simulation set-up are given in the next section.

4.1 Simulation Set-Up

The multi-phase switching simulations were conducted on a PC with a Windows XP operating system. The PC contained an Intel Centrino Duo processor and had a rated clock speed of 1.83 gigahertz. The PC contained 4 gigabytes of random access memory.

The power flow solver from [25] was run using MATLAB version 7.0.1.24704 (R14) Service Pack 1 for Windows machines.

In order to demonstrate the switching algorithm, a new multi-phase bus test system was created from an actual 20-bus system. The original 20-bus case was determined to be unbalanced on phase *C*. Normally closed multi-phase sectionalizing switches were added after each line in the 20-bus system to create a 29-bus test system. Switch placement was not explicitly examined in the solution algorithm. However, comparisons between original or actual bus systems with systems that are created from those systems can be performed to determine if a new switch is needed. For example, with a *SS* inserted after each line, if a switch is never operated then the switch would not be needed and should be "removed". The case created here will not simulate additional tie switches; it does simulate potential new sectionalizing switches.

Since, in this thesis, PHVs are modeled as PQ injections, they can be incorporated into test systems as negative loads thus decreasing the required amount of power at single-phase of the residential load buses. The power would be reduced in the case file in discrete increments using the size of PHV residential systems as a guideline (e.g. <10kW from [9]).

The steps of the solution algorithm were followed and are presented below for reference.

Step 1. Run unbalanced power flow

Step 2. Find the average across the present phases at the buses for variables $|S|$, $|I|$, and $|V|$

Step 3. Find the list of unbalanced buses

Step 4. Rank the list of unbalanced buses

Step 5. Select a new set of open and closed switch operations to be performed (g_k)

Step 6. Repeat Steps 1 – 5 until all lists are within tolerance or stopping criterion is reached

From the problem formulation and solution algorithm chapters the eligibility of the switches was determined by:

1. The initial power flow must solve with no electrical or thermal violations.
2. A radial structure must be observed
3. No load shedding can occur.
4. The minimal number of switch operations must be used.
5. Only same phase- same phase switching is permitted. (ie. Phase *A*- Phase *A*)
6. The transfer current must be less than the spare capacity of the switch $\left(I^{ss} < I^{m}\right)$
7. $I^{SS} < I^{m}_{imbal}$, where I^{m}_{imbal} is the spare imbalance

The base case for this simulation is a 20-bus case. In order to determine if the case is unbalanced the multi-phase switching algorithm was applied to the power flow results of

the initial 20-bus case. The electrical parameter |*S*| was chosen to be examined in the 20-Bus and 29-Bus test cases. The imbalance tolerance for apparent power was chosen to be 2%. The details of the original 20-bus case are presented in the next section.

4.2 Original 20-bus Case

The test system that was used as a basis for the simulation is a 20-bus and 45 node system. Figure 4.1 below is a diagram of the system.

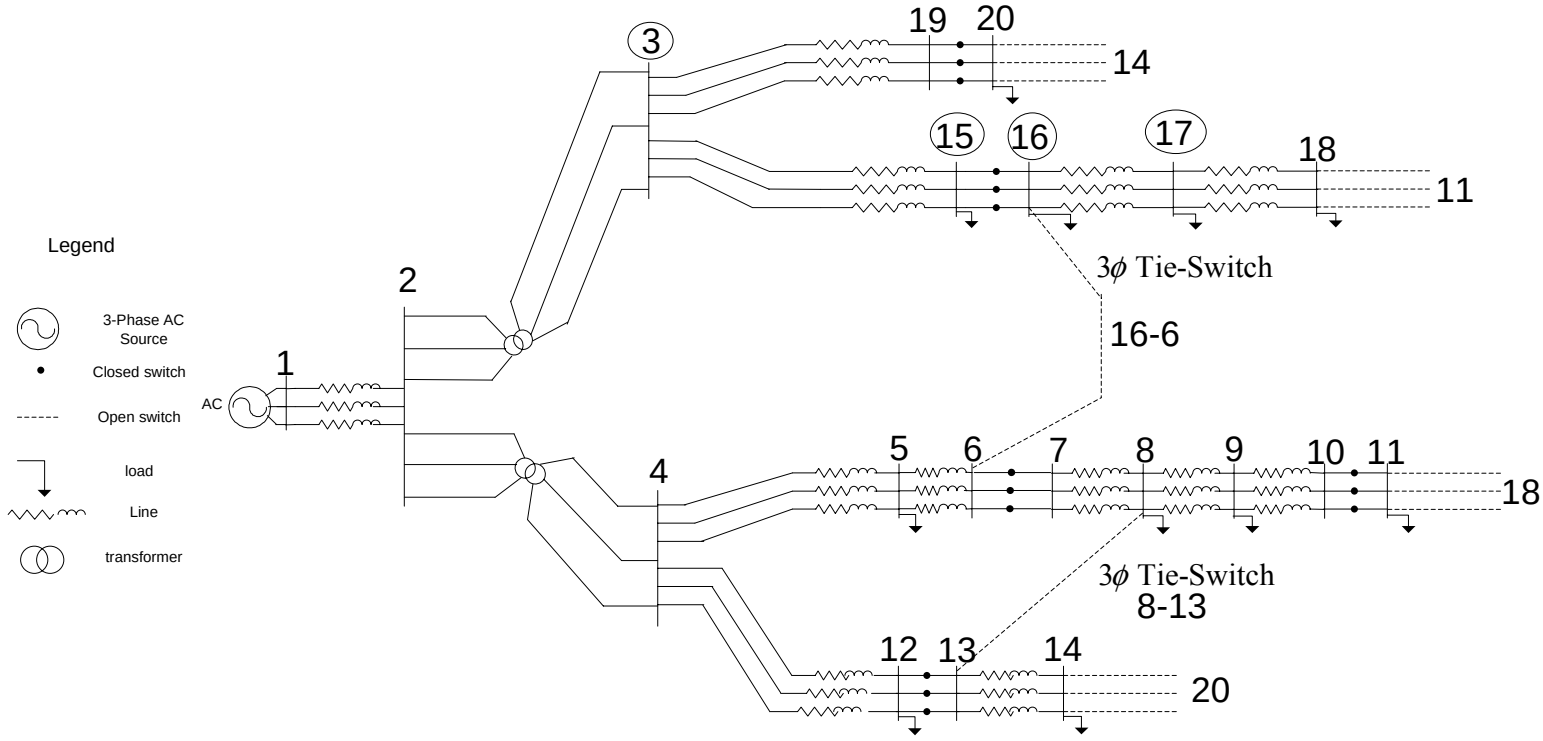

Figure 4.1 20-Bus Original System

In Figure 4.1 there is a substation with three-phase power and two three-phase transformers. A total of nine switches exist, of which four are tie-switches and five are sectionalizing switches. There a total of eleven loads in the 20-bus case. Three loads are unbalanced and eight loads are balanced. Buses *3, 15, 16*, and *17* which are circled were found to be imbalanced for parameters $|S|$ and $|I|$. The specified imbalance tolerances will be listed in Table 4.3. The components in the original system and their count are shown below in Table 4.1.

Table 4.1 Components and Count of 20-Bus System

Component	**Count**
Distribution Lines	12
Sectionalizing Switches	5
Tie Switches	4
Transformers	2
Unbalanced Loads	3
Balanced 3φ Loads	8

The total load of the original 20-bus system is 2736.4 kW and 1985.4 kVAR. The loading by phase is show in Table 4.2 below.

Table 4.2 Total Power Output by Phase for 20-bus System Load Buses

Phase A		**Phase B**		**Phase C**		**Total**	
P	Q	P	Q	P	Q	P	Q
(kW)	(kVAR)	(kW)	(kVAR)	(kW)	(kVAR)	(kW)	(kVAR)
930.38	664.73	886.13	660.24	919.94	660.43	2736.4	1985.4

Columns one through three in Table 4.2 show the power output at phases *A*, *B*, and *C* of the 20-bus system. Each phase's power is separated into real and reactive components. Column four shows the real and reactive power summation for phases *A*, *B*, and *C*. An initial power flow was run on the 20-bus case to ensure that the case was feasible and to obtain initial voltage, current and power results. The 20-bus case was checked for imbalance using the solution algorithm described in Chapter 3. The user specified tolerances for imbalance are shown in the following table.

Table 4.3 User Specified Imbalance Tolerance for 20-bus System

	$\|S\|$	$\|I\|$	$\|V\|$
Tolerance	2%	2%	5%

Table 4.3 lists the user specified tolerance for determining the measure of imbalance for electrical parameters $|S|$, $|I|$, and $|V|$, in the 20-bus case. Bus *3* is a feeder and was determined to have an apparent power imbalance greater than the user specified tolerance. Buses *15, 16*, and *17* were also identified as having a level of imbalance greater than 2% for apparent power. The level of imbalance at these buses is shown in Table 4.4.

Table 4.4 |*S*| % Imbalance for 20-bus System

Bus	**|*S*| % Imbalance**
3	2.933 %
15	4.345 %
16	9.029 %
17	17.976 %

Column one of Table 4.4 lists buses that were identified as exceeding the user specified tolerance for the 20-bus case. Column two lists the |*S*| % imbalance for identified buses. In the next section the test system for the multi-phase switching simulation is presented

4.3 29-Bus Test Case

The following case expands the size of the 20-bus case to a 29-bus case by adding normally closed multi-phase sectionalizing switches after every line. Since, an imbalance was already identified at a transformer on phase *C* of the 20-bus system, no additional PHVs were added to the system. The 29-bus test system is shown below in Figure 4.2.

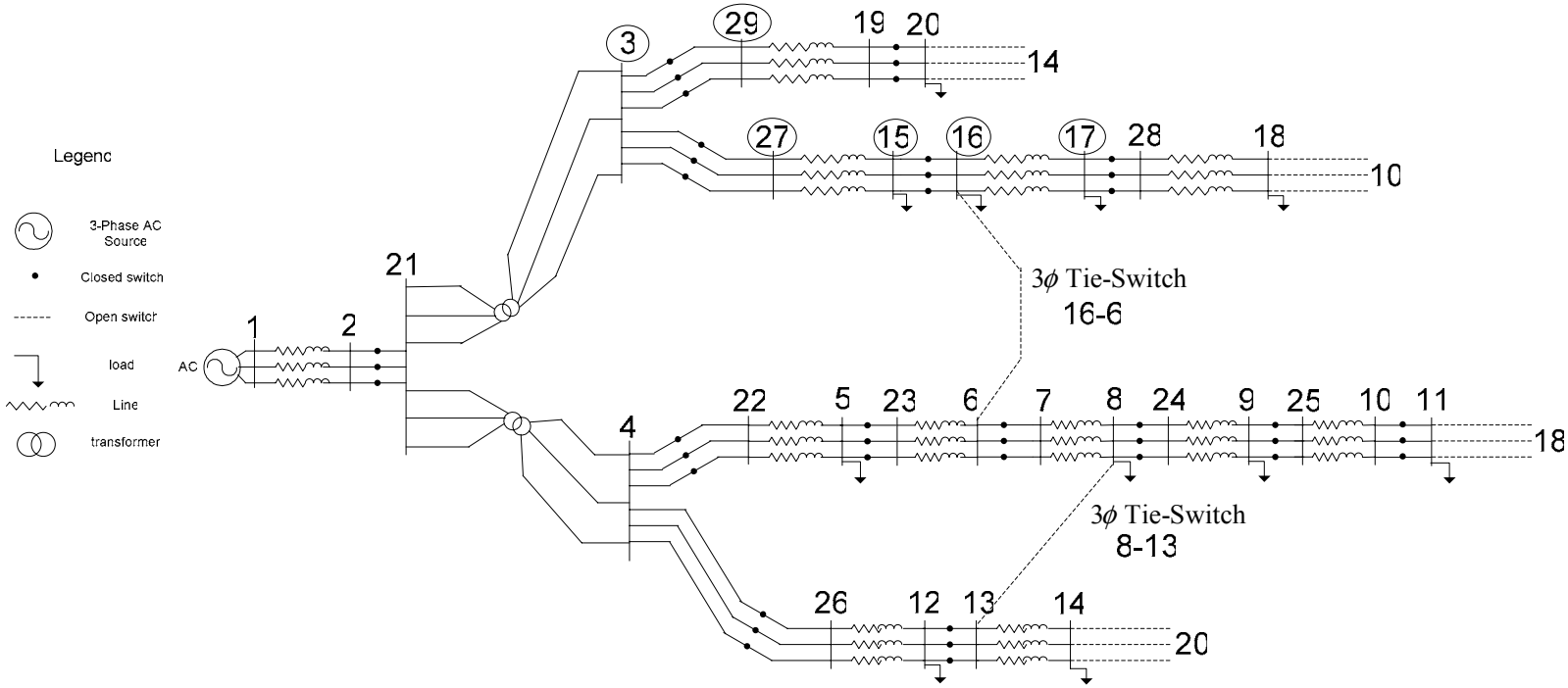

Figure 4.2 29-Bus Test Case

In Figure 4.2 there is a substation with three-phase power and two 3-phase transformers. A total of eighteen switches exist, of which four are tie-switches and fourteen are sectionalizing switches. There a total of eleven loads in the 20-bus case. Three loads are unbalanced and eight loads are balanced. Buses *3*, *15*, *16*, *17*, *27*, and *29* which are circled were found to be imbalanced for parameters $|S|$ and $|I|$. The components and the count for the 29-bus system are given in Table 4.5.

Table 4.5- Components and Count of 29-Bus Test System

Component	**Count**
Distribution Lines	12
Sectionalizing Switches	14
Tie Switches	4
Transformers	2
Unbalanced 3φ Loads	3
Balanced 3φ Loads	8

The total load is the same as the 20-bus case and is 2736.4 kW and 1985.4 kVAR. The load breakdown by phase for the 20-bus case was given in

Table 4.2 and is identical for the 29-bus system. The user specified tolerances to determine the level of imbalance are the same as in Table 4.3. Six buses were determined to have an apparent power imbalance greater than the user specified tolerance. The level of imbalance at these buses is shown in Table 4.6.

Table 4.6 |*S*| % Imbalance for 29-bus System

Bus	**|*S*| % Imbalance**
3	2.933 %
15	4.345 %
16	9.029 %
17	17.976 %
27	2.933 %
29	2.933 %

Column one of Table 4.6 lists buses that were identified as exceeding the user specified tolerance for the 29-bus test case. Column two lists the |*S*| % imbalance for identified buses. Buses *3*, *27* and *29* have a |*S*| % imbalance of 2.933 %. This is expected since a closed multi-phase sectionalizing switch was placed after bus *3* for both of its child branches. When a sectionalizing switch is closed across all phases *A*, *B*, and *C* it behaves as a zero impedance branch. Thus the |*S*| % imbalance seen at buses *3*, *27* and *29* is the same. Bus *17* in Table 4.6 has |*S*| % imbalance of 17.976 %. Bus 17 having the largest |*S*| % imbalance and is the farthest downstream unbalanced bus. Therefore bus *17* is identified as the first imbalanced bus on the unbalanced node lists. Phase *C* of Bus *17* was determined as the imbalanced phase. Thus the unbalanced node is [Bus *17*, Φ*C*].

The load at phases *A*, *B*, and *C* for unbalanced buses *15, 16*, and *17* are shown in Table 4.7.

Table 4.7 Load at Unbalanced Buses in 29-bus Case

	Phase A		Phase B		Phase C	
Bus	P (kW)	Q (kVAR)	P (kW)	Q (kVAR)	P (kW)	Q (kVAR)
15	80.60	102.80	65.60	102.80	80.60	102.80
16	71.63	35.27	61.63	35.26	71.34	35.27
17	34.60	17.57	14.90	13.47	24.60	13.37

In Table 4.7 above, the real and reactive power loads for the unbalanced buses *15, 16*, and *17* are listed. Columns two through four are respectively the loading by phase *A*, *B*, and *C*. Bus *17* has a load that is considerably lower than the load at buses *15* and *16.*

Based on the constraints and analytically determined switching indices, two sectionalizing switch and tie switch pairs out of $\left(2^{18\times3}\right)=\left(2^{54}\right)$ switch combinations were found to be eligible. The results from performing the multi-phase switching algorithm are given in the next section.

4.4 Simulation Results

There are four *TS* in the 29-bus test case. In the following table the *SS*-*TS* eligible pairs for balancing the unbalanced node [Bus *17*, Φ*C*] are listed. The tie-switches are listed horizontally across the table. The sectionalizing switches are listed vertically down the left hand side of the table. An X indicates the eligible *SS*-*TS* pairs.

Table 4.8 – SS-TS Pairs for Balancing Φ*C* of Bus *17, fbus = from bus, tbus = to bus*

Sectionalizing Switch		**Tie Switches**							
		fbus	tbus	fbus	tbus	fbus	tbus	fbus	tbus
fbus	tbus	11	18	6	16	8	13	14	20
15	16	X							
15	16			X					
17	28	X							

Subsequently, bus *3* is chosen for careful examination because it is a transformer bus and it is undesirable to increase the level of imbalance at a transformer. Furthermore the level of imbalance at any upstream bus should not increase because the increase violates the heuristic described in chapter three where the level of system imbalance should not increase. The unbalanced node's |*S*| in per unit and the percentage of reduction of imbalance for the feasible *SS-TS* pairs:

Table 4.9 – % Imbalance for |*S*| at Bus *3* for Pre and Post SS-TS Operation

				Pre- g_k	**Post- g_k**
Sectionalizing Switch		Tie Switch		|S| % Imbal	|S| % Imbal
fbus	tbus	fbus	tbus	**Bus 3**	**Bus 3**
15	16	6	16	2.933 %	11.468 %
15	16	11	18	2.933 %	11.468 %
17	28	11	18	2.933 %	2.772 %

In Table 4.9 the eligible *SS-TS* pairs are listed in the first two columns. Column one, above, lists the bus information for the sectionalizing switch. Column two, lists the bus

information for the corresponding tie-switch. Column three gives the pre-switching % imbalance for |*S*| at bus 3. Column four lists the post-switching % imbalance for |*S*| at bus *3*. The level of imbalance increased at upstream buses for *SS* (15-16) - *TS* (11-18) and *SS* (15-16) - *TS* (6-16). This result is an example of the following constraint $I^{SS} < I^{m}_{imbal}$ (eqn. 3.6.4).

Checking the available difference between the level of imbalance at the TS and I^{SS} ensures that current will not be transferred such that the level of imbalance will increase at the *TS*.

In Table 4.9 the post- g_k |*S*| % imbalance for *SS* (17-28) - *TS* (11-18) pair is 0.161 % less than the pre- g_k apparent power % imbalance. The |*S*| % imbalance at all buses is examined and no new additional buses were found to have an apparent power imbalance greater than the user specified tolerance (2%). Table 4.10 lists the pre-switching and post-switching |*S*| % imbalance for the *SS* (17-28) - *TS* (11-18) pair at the buses identified in the 29-bus test case.

Table 4.10 |S| % Imbalance for 29-bus System

Bus	|S| % Imbalance Pre- g_k	|S| % Imbalance Pre- g_k
3	2.933 %	2.772 %
15	4.345 %	3.707 %
16	9.029 %	0.094 %
17	17.976 %	21.822 %
27	2.933 %	2.772 %
29	2.933 %	2.772 %

Column three gives the pre-switching % imbalance for |*S*| at the identified imbalanced buses for the 29-bus test case. Column four lists the post-switching % imbalance for |*S*| at previously identified imbalanced buses for the 29-bus test case. Now, only five buses have an apparent power imbalance greater than the user specified tolerance. It is observed that bus 6 has a pre-switching |*S*| % imbalance of 9.029 %. Post-switching the |*S*| % imbalance is 0.094 %. Bus *6* as a result of switching (17-28) - *TS* (11-18) pair now has an apparent power imbalance less than the user specified tolerance. However, examination of Bus *17* shows the |*S*| % imbalance has increased from 17.976% to 21.822 %. This increase violates the heuristic described in chapter three; level of system imbalance cannot increase. Thus all *SS*-*TS* pair results are discarded. Still, it is important to note that the load at bus *17* is small (from Table 4.7) and the % imbalance looks much larger in comparison to the amount of watts that are being transferred.

In the next section, the observations for the multi-phase switching results are presented.

4. 5 Observations

It is observed that the multi-phase switching for phase balancing algorithm did not decrease the level of imbalance for |*S*| phase *C* of bus *17*. The increase in level of imbalance at bus *17* was expected because the loading at bus 17 is very low in watts. However, the level of imbalance at five buses upstream was decreased. In addition, bus 6's level of imbalance was reduced significantly enough to become within the user specified tolerance.

The heuristic described in chapter three where the level of system imbalance should not increase should be relaxed to take into account the difference between the number of unbalanced buses and the size of imbalance. In the 29-bus case the buses upstream of the unbalanced bus became less unbalanced. This improvement is significant in comparison to the increase in level of imbalance seen at the unbalanced node because the loading at the unbalanced node is small. Some guidelines regarding the trade-off between the size of imbalance and the number of unbalanced buses should be established. It is recognized that a larger test case may have very different results. The results would differ because the network topology would change which may allow for a greater number of switches and thus a greater number of SS-*TS* pairs.

In the next section, the summary for the simulation results is given.

4. 6 Summary

The multi-phase switching algorithm did not reduce the percentage of imbalance seen at the unbalanced node [Bus 17, φC]. In addition, the level of imbalance was seen to decrease at upstream buses in the system.

In the future, one may need to adjust the switching decision schemes to be more elaborate. All possible sectionalizing switches have been added to the 29-bus test case. Thus, further investigation would be conducted for tie switch placement. Else, capacitor placement or other solutions would be investigated. Careful consideration would need to be given to capacitor placement and other solutions because of their drawbacks which were discussed in Chapter 1.

The simulation results were generated manually and there is an understanding that there may be some small discrepancies due to mutual coupling. However, the power flow Jacobian is shown to be diagonally dominant in [30] and thus the impacts due to mutual coupling are expected to be marginal. Still, the discrepancy does not affect how the multi-phase switching problem would be solved.

The conclusion and future work sections are presented in the next chapter.

Chapter 5. Conclusion

This thesis presented the concept of multi-phase network reconfiguration in order to address expected challenges in distribution systems, specifically, increased imbalance from various DER installations. Select component models, imbalance indices, a problem formulation, a solution algorithm based on analytical indices and simulation results for the multi-phase switching problem were presented. This work quantified the level of imbalance and examined a switching algorithm to correct the level of imbalance from the average at buses.

In this investigation, the penalty function method was used to handle constraints of the optimization problem. The multi-phase switching algorithm employed greedy search and memory based heuristics utilizing analytically determined indices for imbalance to perform network reconfiguration. Lastly, simulation results were presented for the multi-phase switching with uncertain loads problem using a 29-bus test system.

The results showed that the multi-phase switching algorithm was able to reduce the level of imbalance at upstream buses in a radial system, but it was not able to reduce the percentage of imbalance seen at each bus or all targeted buses. The reduction of imbalance at upstream buses is a significant improvement in the systems level of imbalance. In this particular example, the increase in level of imbalance seen at one unbalanced bus was not severe because the loading at the unbalanced bus was small. Further consideration regarding the trade-off between the size of imbalance and the number of unbalanced buses is needed.

5.2 Summary of Research Contributions

Specifically, this thesis discussed and presented the following:

- electrical parameters $|S|$, $|V|$, and $|I|$ were examined to determine a measure of imbalance for phase balancing
- the concept of using multi-phase switching was proposed
- a multi-phase switch model and a multi-phase switching power flow algorithm to determine all eligible switch pairs was presented
- an investigation of balancing the real power output across a bus using the proposed switch algorithm was conducted

5.3 Future Work

Several open issues remain with respect to the multi-phase switching problem. First, stemming from this thesis, the simulation results were generated manually and there is an understanding that there may be some small discrepancies due to mutual coupling. While these impacts are expected to be marginal, a formalized implementation should be completed. Second, different imbalance indices can be identified and studied. Also, a common network reconfiguration objective to minimize the real power loss has been relaxed in this investigation and was viewed as a byproduct of the other objectives. In future work, this objective can be included and new switching schemes can be developed.

List of References

1. ANSI Standard C84.1, American National Standard for Electric Power Systems and Equipment—Voltage Ratings (60 Hertz), 2006, Annex 1

2. Aoki, K. et. al., "An Efficient Algorithm for Load Balancing of Transformers and Feeders By Switch Operation in Large Scale Distribution Systems," IEEE Transactions on Power Delivery, Vol. 3, No. 4, October 1998, pp. 1865-1872.

3. Baran, M. and Wu, F., "Network Reconfiguration in Distribution Systems for Loss Reduction and Load Balancing," IEEE Transactions on Power Delivery, Vol. 4, No. 2, April 1989, pp. 1401-1407.

4. Bergen Arthur R. and Vittal Vijay. Power Systems Analysis. 2nd ed. Upper Saddle River: Prentice Hall, 2000.

5. Chapman, Stephen J. Electric Machinery Fundamentals. 4th ed. Boston: McGraw Hill, 2005.

6. Chiang, H.D. and Jean-Jumeau, R., "Optimal Network Reconfiguration in Distribution Systems: Part 1: A New Formulation and A Solution Methodology," IEEE Transactions on Power Delivery, Vol. 5, No. 4, November 1990, pp. 1902-1909.

7. Chiang, H.D. and Jean-Jumeau, R., "Optimal Network Reconfiguration in Distribution Systems: Part 2: Solution Algorithms and Numerical Results," IEEE Transactions on Power Delivery, Vol. 5, No. 3, July 1990, pp. 1568-1574.

8. Chuang, Y.C. et.al., "Rule-Expert Knowledge-Based Petri Net Approach for Distribution System Temperature Adaptive Feeder Reconfiguration," IEEE Transactions on Power Systems, Vol. 21, No. 3, August 2006, pp. 1362-1370.

9. Golder, A. S., “Photovoltaic Generator Modeling for Large Scale Distribution System Studies,” Masters Dissertation, Drexel University, Oct. 2006

10. Hsu, Y.Y. et.al., “Transformer and Feeder Load Balancing Using A Heuristic Search Approach,” IEEE Transactions on Power Systems, Vol. 8, No. 1, Februrary 1993, pp. 184-190.

11. Ishikawa,T., "Grid-connected photovoltaic power systems: Survey of inverter and related protection equipments," International Energy Agency (IEA), Tokyo Japan, Tech. Rep. IEA-PVPS T5-05: 2002, December, 2002.

12. Ke, Y.L. et.al., “Power Distribution System Switching Operation Scheduling for Load Balancing by Using Colored Petri Nets,” IEEE Transactions on Power Systems, Vol. 19, No. 1, Februrary 2004, pp. 629-635.

13. Liu, C.C. et.al., “Loss of Minimization of Distribution Feeders: Optimality and Algorithms,” IEEE Transactions on Power Delivery, Vol. 4, No. 2, April 1989, pp. 1281-1289.

14. McDonald, J., Bruning A.M., and Mahieu,W.R., “Cold load pickup,” IEEE Transactions on Power Apparatus and Systems, Vol. PAS-98, July/August 1979, pp. 1384-1386

15. Miu, K. and Chiang, H.D., “ Capacitor Placement, Replacement, and Control in Large – Scale Distribution Systems by GA-Based Two-Stage Algorithm,” IEEE Transactions on Power Systems, Vol. 12, No. 3, August 1997, pp. 1160-1166.

16. Miu, K. and Chiang, H.D., “Service Restoration for Unbalanced Radial Distribution Systems with Varying Loads: Solution Algorithm,” Power Engineering Society Summer Meeting, Vol. 1, July 1999, pp.254 - 258

17. Miu, K. and Chiang, H.D., "Electric Distribution System Load Capability: Problem Formulation, Solution Algorithm, and Numerical Results," IEEE Transactions on Power Delivery, Vol. 15, No. 1, January 2000, pp.436-442

18. P.Pillay and M. Manyage, "Derating of Induction Motors Operating With a Combination of Unbalance Voltages and Over or Undervoltages," IEEE Transactions on Energy Conversion, Vol. 17, No. 4, pp. 485-491, Dec. 2002

19. P.Pillay and M. Manyage, "Loss of Life in Induction Machines Operating With Unbalanced Supplies," IEEE Transactions on Energy Conversion, Vol. 21, No. 4, pp. 813-822, Dec. 2006

20. Taylor, T. and Lubkeman, D., "Implementation of Heuristic Search Strategies for Distribution Feeder Reconfiguration," IEEE Transactions on Power Delivery, Vol. 5, No. 1, January 1990, pp. 239-246.

21. Ucak, C. and Pahwa, A. "An analytical Approach To Step-by-Step Restoration of Distribution Systems Following Extended Outages," IEEE Transactions on Power Delivery, Vol. 9, No. 3, July 1994, pp.1717-1723

22. Wakileh, J. and Pahwa, A. "Optimization of distribution system design to accommodate cold load pickup," IEEE Trans. Power Delivery, vol. 12, pp. 339–345, Jan. 1997.

23. Wakileh, J. and Pahwa A., "Distribution System Design Optimization for Cold Load Pickup," IEEE Transactions on Power Systems, Vol. 11, No. 4, November 1996, pp. 1879-1884

24. Wang, J.C. et.al., "Efficient Algorithm for Real-Time Network Reconfiguration in Large Scale Unbalanced Distribution Systems," IEEE Transactions on Power Systems, Vol. 11, No. 1, Februrary 1996, pp. 511-517.

25. Wood Allen J., and Wollenberg Bruce F. Power Generation Operation and Control. 2nd ed. New York: Wiley Interscience. 1996.

26. Wu, J.S. et.al., "A Heuristic Search Approach to Feeder Switching Operations for Overload, Faults, Unbalanced Flow and Maintenance," IEEE Transactions on Power Delivery, Vol. 6, No. 4, October 1991, pp. 1579-1585.

27. Wu, J.S. et.al., "A Petri Net Algorithm for Scheduling of Generic Restoration Actions," IEEE Transactions on Power Systems, Vol. 12, No. 1, Februrary 1997, pp. 69-76.

28. Zhou,Q. et.al., "Distribution Feeder Reconfiguration for Service Restoration and Load Balancing," IEEE Transactions on Power Systems, Vol. 12, No. 2, May 1997, pp. 724-729.

29. Zimmerman R. , and Chiang, H.D. , "Transformer modeling using line-to-line voltages in ungrounded power distribution networks," IEEE PES Transmission and Distribution Conference and Exposition, Vol. 3, September 2003, pp.1033-1036

30. Zimmerman R. , and Chiang, H.D. , "Fast Decoupled Power Flow for Unbalanced Radial Distribution Systems," IEEE Transactions on Power Delivery, Vol. 10, No. 4, November 1995, pp.2045-2052

31. Zimmerman R., "Comprehensive Distribution Power Flow: Modeling, Formulation, Solution Algorithms and Analysis," PhD Dissertation, Cornell University, Jan. 1995

32. http://www.energy.siemens.com/cms/us/US_Products/Portfolio/PTIPSSoftware/Pages/PSSE.aspx,. Siemens. August 23, 2008. keyword "PSSE."

33. http://www.pseg.com/customer/solar.jsp, Public Service Electric and Gas (PSEG). August 15, 2008

34. http://www.atlanticcityelectric.com/energy/renewable/default.aspx, Atlantic City Electric (AEC). August 15, 2008.

35. http://www.atlanticcityelectric.com/energy/renewable/nj/, Atlantic City Electric (AEC). August 15, 2008.